Inorganica Chimica Acta 483 (2018) 411–424

Contents lists available at ScienceDirect

Inorganica Chimica Acta

journal homepage: www.elsevier.com/locate/ica

Research paper

Temperature-dependent elongation of the H—H bond in dihydrogen complexes of Ru(II) bearing an NHC ligand: Effect of the NHC and *trans* ligands

Deep Mala, Balaji R. Jagirdar*, Yogesh P. Patil, Munirathinam Nethaji

Department of Inorganic & Physical Chemistry, Indian Institute of Science, Bangalore 560012, India

ARTICLE INFO

Keywords:
N-heterocyclic carbene
Ruthenium complexes
Dihydrogen complexes
Trans ligands
H—H bond distances

ABSTRACT

Ruthenium hydride complexes bearing an N-heterocyclic carbene ligand [RuHCl(CO)(IMes)(PPh_3)(L/L′)] (L = py, **2**; 4Mepy, **3**; L′ = MeCN, **4**; Me_3CCN, **5**) have been synthesized in high-yields via reaction of [RuHCl(CO)(IMes)(PPh_3)] (**1**) with pyridyl ligands L (L = py and 4Mepy) or nitrile ligands L′ (L′ = MeCN and Me_3CCN). The ligands L/L′ are labile in all the ruthenium hydride complexes; they can be easily replaced by Lewis bases. The X-ray structures of complexes **2** and **3** show intramolecular π-π interactions between the aromatic ring of PPh_3, IMes, and pyridyl ligands. The protonation reaction of **2–5** gives the corresponding dihydrogen complexes of the type [RuCl(η^2-H_2)(CO)(IMes)(PPh_3)(L/L′)][OTf] complexes (L = py, **6**; 4Mepy, **7**; L′ = MeCN, **8**; Me_3CCN, **9**). In all the dihydrogen complexes, H—H bond distances of η^2-H_2 ligand is temperature-dependent: 0.98 Å to 0.93 Å in the temperature range of 183–233 K. Attempts to synthesize analogous ruthenium hydride complexes bearing phosphine ligands resulted in a mixture of *cis* and *trans*-[RuHCl(CO)(PPh_3)$_2$(L)] [L = py, **10/11** ($trans_{HCl}/cis_{HCl}$); 4Mepy, **12/13** ($trans_{HCl}/cis_{HCl}$)] complexes. A comparative study has been done to get an insight into the temperature-dependent H—H bond distances in complexes **6–8** by synthesizing analogous ruthenium dihydrogen complexes, [RuCl(η^2-H_2)(CO)(PPh_3)$_2$(L)](OTf) (L = py, **15**; 4Mepy, **17**). All the complexes have been characterized using NMR spectroscopy. The X-ray crystal structures of complexes **2**, **3**, and **12** have also been determined.

1. Introduction

The study of ruthenium hydride and dihydrogen complexes is of great interest in the field of homogeneous catalysis [1,2]. These complexes play a crucial role in catalysis as reactive intermediates, catalysts, and catalyst precursors [3]. A large number of catalytic reactions have been reported using these complexes by several research groups [2,4]. In particular, dihydrogen complexes are one of the most interesting classes of compounds because of their resemblance to sigma complexes [5–7]. Among different classes of dihydrogen complexes, the chemistry of ruthenium dihydrogen complexes bearing phosphine ancillary ligands has been explored extensively [6,8].

The successful isolation of an N-heterocyclic carbene (NHC) by Arduengo in 1991 opened up a new class of ligands to investigate their transition metal chemistry [9]. The strong metal-carbon bond in metal complexes bearing NHC ligands makes these complexes thermally stable [10]. The first ruthenium NHC dihydrogen complex was reported by Leitner and co-workers in 2003 [11]. Few other metal dihydrogen complexes containing NHC as ancillary ligands have also been reported to date [1e,12].

In general, the nature of ancillary ligands in dihydrogen complexes has a significant influence on their H—H bond distances [5f,7a,13]. D'Agostino and co-workers reported the synthesis of ruthenium complexes [RuX(H_2)($R_2PCH_2CH_2PR_2$)$_2$](PF_6) (X=Cl, H; R=Ph, Et) and also studied the influence of ligands, chloride as well as hydride, on the H—H bond distances [13]. Spin-lattice relaxation time (T_1) and H, D coupling constant ($^1J_{HD}$) data indicate that the H-H distance in the chloride complex was longer as compared to the hydride complex. Similarly, Jagirdar and co-workers studied the influence of the electronic properties of phosphine co-ligands in the ruthenium dihydrogen complexes [RuCl(H_2)($ArCH_2$)$_2$$PCH_2CH_2P$($CH_2Ar$)$_2$]($BF_4$) (Ar=*p*-$FC_6H_4$, C_6H_5, *m*-MeC_6H_4, *p*-MeC_6H_4, *p*-$^iPrC_6H_4$). They reported that the electron donating nature of Ar group of the phosphine ligands results in a small increment in the H—H bond distance (0.97– 1.03 Å) [7a]. We recently reported that two [RuHCl(CO)(IMes)(PPh_3)] fragments (**1**) bridged by 4,4′-bipyridine, 1,2-bis(4-pyridyl)ethylene, and 1,2-bis(4-

* Corresponding author.
E-mail address: jagirdar@iisc.ac.in (B.R. Jagirdar).

https://doi.org/10.1016/j.ica.2018.08.015
Received 4 July 2018; Received in revised form 15 August 2018; Accepted 15 August 2018
Available online 19 August 2018

pyridyl)ethane ligands form stable hydride complexes [{RuHCl(CO)(IMes)(PPh_3)}$_2$(NN)] [NN = 4,4′-bipyridyl, 1,2-bis(4-pyridyl)ethylene, 1,2-bis(4-pyridyl)ethane] [14]. Subsequently, protonation of these bimetallic hydride complexes resulted in the corresponding dihydrogen complexes [14]. However, the influence of IMes on the properties of those bimetallic complexes could not be established. Herein, we present a comparative study of the dihydrogen complexes bearing IMes, PPh_3, and different ligands *trans* to the bound H_2 ligands.

2. Experimental

2.1. Materials and methods

All manipulations were carried out using standard Schlenk techniques under N_2 or Ar atmosphere. Solvents were dried using calcium hydride (dichloromethane, acetonitrile, and pyridine), sodium benzophenone ketyl (hexanes, pentane, toluene, THF, and Et_2O) and distilled under N_2 or Ar atmosphere just before use. HOTf, DOTf, $CDCl_3$, tol-d_8, pyvalonitrile (Me_3CCN), and 4-methylpyridine were used as received from Sigma-Aldrich. CD_2Cl_2 was dried and distilled over calcium hydride and degassed by two consecutive cycles of freeze-pump-thaw. Synthesis of 1,3-bis(2,4,6-trimethylphenyl)imidazol-2-ylidene (IMes) [15] and [RuHCl(CO)(PPh_3)$_3$] [16], [RuHCl(CO)(IMes)(PPh_3)] [3a] were carried out by following literature procedures. NMR spectra were obtained using an Avance Bruker 400 MHz spectrometer. ^{1}H and ^{13}C{^{1}H} NMR (100 MHz) spectra were referenced to the residual proton signal of the deuterated solvents (5.32 ppm, CD_2Cl_2; 7.26 ppm, $CDCl_3$; 2.08 ppm, tol-d_8) and carbon signal of the deuterated solvents (53.84 ppm, CD_2Cl_2; 77.16 ppm, $CDCl_3$), respectively. The ^{31}P{^{1}H} NMR spectra (161 MHz) were referenced to 85% H_3PO_4 (0.0 ppm, external standard). IR spectra were recorded using a Bruker Alpha FTIR spectrometer and elemental analyses were obtained using Thermo Finnigan Flash EA 1112 CHN analyzer.

2.2. Synthesis and characterization of [RuHCl(CO)(IMes)(PPh_3)(L/L′)] (L = py, **2**; 4Mepy, **3**; L′ = MeCN, **4**; Me_3CCN, **5**)

2.2.1. Synthesis of [RuHCl(CO)(IMes)(PPh_3)(L)] (L = py, **2**; 4Mepy, **3**)

Pyridine (py) or 4-methylpyridine (4Mepy) (1.5 mL) was added to [RuHCl(CO)(IMes)(PPh_3)] (**1**) (275 mg, 0.37 mmol) at room temperature and stirred for 1 min. The product was obtained via precipitation by addition of 15 mL of hexanes. The resulting pale yellow colored complexes were isolated in high yields (260 mg, 85%, **2**; 285 mg, 90%, **3**) through filtration and washed twice with 5 mL of hexanes and dried under vacuum. The ^{1}H, ^{31}P{^{1}H} NMR spectra were recorded at 293 K and 198 K. The ^{13}C{^{1}H} NMR spectrum was recorded at room temperature.

2.2.2. Synthesis of [RuHCl(CO)(IMes)(PPh_3)(MeCN)] (**4**)

A solution of IMes (200 mg, 0.66 mmol) in 8 mL of toluene was added to a suspension of [RuHCl(CO)(PPh_3)$_3$] (420 mg, 0.44 mmol) in 8 mL of toluene. The reaction mixture was stirred at 303 K for 2 h. The reaction mixture was concentrated up to 5 mL and filtered through a filter frit. The filtrate was concentrated up to 0.5 mL under vacuum and 15 mL of hexanes was added. Upon cooling this solution in a low-temperature bath (liq. N_2 and acetone) and stirring for 5 min, a precipitate of orange-yellow colored complex **1** was obtained. The supernatant was removed under a stream of N_2 gas. Complex **1** was washed with cold hexanes (2 × 4 mL) and dried under vacuum. MeCN (0.3 mL) was added to complex **1** at room temperature and stirred for 1 min. Addition of 10 mL of Et_2O gave an off-white precipitate of [RuHCl(CO)(IMes)(PPh_3)(MeCN)] (**4**) which was washed with 5 mL of Et_2O. The product was washed again using Et_2O (2 × 5 mL) and dried under vacuum (yield = 170 mg, 59%). The ^{1}H, ^{31}P{^{1}H} (293 K) and ^{13}C{^{1}H} NMR (room temperature) spectra of complex **4** were recorded and the data have been summarized below.

2.2.3. Synthesis of [RuHCl(CO)(IMes)(PPh_3)(Me_3CCN)] (**5**)

Me_3CCN (0.3 mL) was added to complex **1** (275 mg, 0.37 mmol) at room temperature and stirred for 1 min. The product was washed using hexanes (10 mL). The resulting off-white colored product of [RuHCl(CO)(IMes)(PPh_3)(Me_3CCN)] complex (**5**) was washed twice with 5 mL of hexanes and dried under vacuum (isolated yield = 250 mg, 87%). The ^{1}H, ^{31}P{^{1}H}, and ^{13}C{^{1}H} NMR spectra data of complex **5** have been summarized below.

2.2.4. Variable temperature (VT) NMR study of **2**, **3**, **4**, and **5**

Complexes **2–5** [20 mg, **2**; 21 mg, **3**; 19 mg, **4**; 20 mg, **5** (each of 0.025 mmol)] were dissolved in 0.5 mL of CD_2Cl_2 in Schlenk NMR tubes and the solutions were degassed by two freeze–pump-thaw cycles. The NMR tubes were then flame-sealed under vacuum and then inserted into an NMR probe at 293 K. The ^{1}H and ^{31}P{^{1}H} NMR spectra were recorded at each 5 or 10 K temperature interval (293–198 K). The complete ^{1}H, ^{31}P{^{1}H} NMR spectral data acquired at 198 K are given in Table 1 and^1 H, ^{31}P{^{1}H}, ^{13}C{^{1}H} NMR and IR spectral data obtained at 293 K are summarized below.

2.2.5. Characterization data of [RuHCl(CO)(IMes)(PPh_3)(py)] (**2**)

^{1}H NMR (CD_2Cl_2, 293 K, ppm): δ = 8.50 (br s, 1H, py), 8.00 (br s, 1H, py), 7.00–7.21 (m, 15H, P*Ph*$_3$; 1H, py; s, 2H, IMes *m*-C*H*), 6.81 (s, 2H, IMes *m*-C*H*), 6.62 (s, 2H, NC*H* = C*H*N), 6.53 (br s, 2H, py), 2.28 (s, 6H, IMes *p*-C*H*$_3$), 2.24 (s, 6H, IMes *o*-C*H*$_3$), 2.10 (s, 6H, IMes *o*-C*H*$_3$), −13.28 (d, $^2J_{HP}$ = 15.5 Hz, 1H, Ru–*H*). **^{31}P{^{1}H} NMR** (CD_2Cl_2, 293 K, ppm): δ = 46.2 (s, 1P, *P*Ph$_3$). **^{13}C{^{1}H} NMR** (CH_2Cl_2; $CDCl_3$ ext. lock, ppm): δ = 204.2 (d, $^2J_{CP}$ cis = 13.6 Hz, *C*O), 186.5 (d, $^2J_{CP}$ trans = 102.0 Hz, IMes N*C*N), 149–153 (br. m, py),138.4 (s, IMes), 137.9 (s, IMes), 136.2 (s, IMes), 136.1 (s, IMes), 135.5 (d, $^1J_{CP}$ = 36.0 Hz, *i*-P*Ph*$_3$), 134.0 (d, $^2J_{CP}$ = 10.0 Hz, *o*-P*Ph*$_3$), 128.5 (s, IMes), 128.4 (s, IMes), 128.4 (s, *p*-P*Ph*$_3$), 127.2 (d, $^3J_{CP}$ = 9.0 Hz, *m*-P*Ph*$_3$), 123.1 (s, IMes NCH=*C*HN), 123.0 (s, IMes), 20.9 (s, IMes *p*-*C*H$_3$), 18.5 (s, IMes *o*-*C*H$_3$), 18.4 (s, IMes *o*-*C*H$_3$). IR (cm^{-1}): ν(CO) 1877. Anal. calcd for $C_{45}H_{45}ClN_3OPRu$ (811), C: 66.61, H: 5.59, N: 5.18. found: C: 66.47, H: 5.62, N: 4.99.

2.2.6. Characterization data of [RuHCl(CO)(IMes)(PPh_3)(4Mepy) (**3**)

^{1}H NMR (CD_2Cl_2, 293 K, ppm): δ = 8.21 (br. s, 1H, 4Mepy *o*-C*H*), 7.95 (br. s, 1H, 4Mepy *o*-C*H*), 7.00–7.22 (m, 15H, P*Ph*$_3$, 2H, IMes *m*-C*H*), 6.83 (s, 2H, IMes *m*-C*H*), 6.65 (s, 2H, NC*H*=C*H*N), 6.37 (br. s, 2H, 4Mepy *m*-C*H*), 2.29 (s, 6H, IMes *p*-C*H*$_3$), 2.25 (s, 6H, IMes *o*-C*H*$_3$), 2.18 (s, 3H, 4Mepy *p*-C*H*$_3$), 2.10 (s, 6H, IMes *o*-C*H*$_3$), −13.19 (br. s, 1H, Ru-*H*). **^{31}P{^{1}H} NMR** (CD_2Cl_2, 293 K, ppm): δ = 46.4 (s, 1P, *P*Ph$_3$). **^{13}C{^{1}H} NMR** (CH_2Cl_2; $CDCl_3$ ext. lock, ppm): δ = 204.3 (d, $^2J_{CP}$ cis = 13.6 Hz, *C*O), 186.4 (d, $^2J_{CP}$ trans = 102.0 Hz, IMes N*C*N), 150.1–153.0 (br. m, 4Mepy), 138.5 (s, IMes), 138.0 (s, IMes), 136.3 (s, IMes), 136.1 (s, IMes), 135.6 (d, $^1J_{CP}$ = 36.0 Hz, *i*-P*Ph*$_3$), 134.1 (d, $^2J_{CP}$ = 10.0 Hz, *o*-P*Ph*$_3$), 128.5 (s, IMes), 128.4 (s, IMes), 128.4 (s, *p*-P*Ph*$_3$), 127.1 (d, $^3J_{CP}$ = 9.0 Hz, *m*-P*Ph*$_3$), 123.9 (s, IMes NCH=*C*HN), 123.1 (s, IMes NCH=*C*HN), 20.9 (s, IMes *p*-*C*H$_3$), 18.5 (s, IMes *o*-*C*H$_3$), 18.4 (s, IMes *o*-*C*H$_3$), 20.5 (s, 4Mepy *p*-*C*H$_3$). IR (cm^{-1}): ν(CO) 1874. Anal. calcd for $C_{46}H_{47}ClN_3OPRu$ (825), C: 66.94, H: 5.74, N: 5.09. found: C: 66.91, H: 5.94, N: 5.21.

2.2.7. Characterization data of [RuHCl(CO)(IMes)(PPh_3)(MeCN)] (**4**)

^{1}H NMR (CD_2Cl_2, 293 K, ppm): δ = 7.21–7.36 (m, 15H, P*Ph*$_3$), 7.07 (s, 2H, IMes *m*-C*H*), 7.04 (s, 2H, NC*H* = C*H*N), 6.97 (s, 2H, IMes *m*-C*H*), 2.36 (s, 6H, IMes *p*-C*H*$_3$), 2.30 (s, 6H, IMes *o*-C*H*$_3$), 2.19 (s, 6H, IMes *o*-C*H*$_3$), 1.42 (s, 3H, *Me*CN), −15.97 (br. s, 1H, Ru-*H*). **^{31}P{^{1}H} NMR** (CD_2Cl_2, 293 K, ppm): δ = 44.6 (s, 1P, *P*Ph$_3$). **^{13}C{^{1}H} NMR** (CH_2Cl_2; $CDCl_3$ ext. lock, ppm): δ = 203.0 (d, $^2J_{CP}$ cis = 13.5 Hz, *C*O), 186.9 (d, $^2J_{CP}$ trans = 102.5 Hz, IMes N*C*N), 138.5 (s, IMes), 138.1 (s, IMes), 137.0 (s, IMes), 136.7 (s, IMes), 135.6 (d, $^1J_{CP}$ = 37.0 Hz, *i*-P*Ph*$_3$), 134.4 (d, $^2J_{CP}$ = 10.7 Hz, *o*-P*Ph*$_3$), 128.8 (s, *p*-P*Ph*$_3$), 128.5 (s, IMes), 128.4 (s, IMes), 127.4 (d, $^3J_{CP}$ = 9.0 Hz, *m*-P*Ph*$_3$), 122.9 (s, IMes NCH=*C*HN),

Table 1
^{1}H and ^{31}P{ ^{1}H} NMR spectral data of [RuHCl(CO)(IMes)(PPh_3)(L/L′)] (L = py, **2**; 4Mepy, **3**; L′ = MeCN, **4**; Me_3CCN, **5**) in CD_2Cl_2 at 198 K.

Complexes	, ^{1}H (ppm)				δ,^{31}P{^{1}H} (ppm)
	(Ru-*H*)	(L/L′)	(IMes)	(PPh_3)	(PPh_3)
2	−13.03 (d, $^{2}J_{H,P}$ = 20.0 Hz)	8.05 (d, $^{3}J_{H,H}$ = 5.2 Hz, 1H, *o*-C*H*), 7.97 (d, $^{3}J_{H,H}$ = 5.2 Hz, 1H, *o*-C*H*) 7.00–7.17 (m, 1H, *p*-C*H*), 6.49, 6.27 (t, $^{3}J_{H,H}$ = 6.3 Hz, 2H, *m*-C*H*)	7.00–7.17 (m, 1H, *m*-C*H*), 6.44 (s, 1H, NC*H*=C*H*N), 6.02 (s, 1H, NC*H*=C*H*N), 2.44 (s, 3H, *p*-CH_3), 2.39 (s, 3H, *p*-CH_3), 2.11, 2.07 (s, 6H, *o*-CH_3), 1.93, 191 (s, 6H, *o*-CH_3)	7.00–7.17 (m, 15H)	47.6 (s)
3	−13.02 (d, $^{2}J_{H,P}$ = 20.0 Hz)	7.85 (d, $^{3}J_{H,H}$ = 5.4 Hz, 1H, *o*-C*H*), 7.79 (d, $^{3}J_{H,H}$ = 5.4 Hz, 1H, *o*-C*H*), 6.35, 6.08 (d, $^{3}J_{H,H}$ = 5.0 Hz, 2H, *m*-C*H*), 2.11 (s, 3H, *p*-CH_3)	7.02–7.16 (m, 3H, *m*-C*H*), 6.89 (s, 1H, *m*-C*H*), 6.46 (s, 1H, NC*H*=C*H*N), 6.10 (s, 1H, NC*H*=C*H*N), 2.44 (s, 3H, *p*-CH_3), 2.40 (s, 3H, *p*-CH_3), 2.11, 2.08 (s, 6H, *o*-CH_3), 1.96, 1.91 (s, 6H, *o*-CH_3)	7.02–7.16 (m, 15H)	47.7 (s)
4	−12.58 (d, $^{2}J_{H,P}$ = 20.0 Hz)	1.11 (s, 3H, CH_3)	7.00 (s, 2H, *m*-C*H*), 6.98 (s, 2H, NC*H*=C*H*N), 6.89 (s, 2H, *m*-C*H*), 2.36 (s, 6H, *p*-CH_3), 2.31 (s, 3H, *o*-CH_3), 2.22 (s, 3H, *o*-CH_3), 2.13, 196 (s, 6H, *o*-CH_3)	7.21–7.36 (m, 15H)	46.2 (s)
5	−12.91 (d, $^{2}J_{H,P}$ = 19.3 Hz)	0.58 (s, 9H, C(CH_3)$_3$)	6.98–7.29 (br. m, 4H, *m*-C*H*, 2H, NC*H*=C*H*N), 2.36 (m, 18H, CH_3)	6.98–7.29 (m, 15H)	41.1 (s)

116.9 (s, MeCN *C*N), 21.0 (s, IMes *p*-CH_3), 18.6 (s, IMes *o*-CH_3), 18.4 (s, IMes *o*-CH_3), 2.4 (s, MeCN CH_3,). IR (cm^{-1}): ν (CO) 1888 (KBr).

*2.2.8. Characterization data of [RuHCl(CO)(IMes)(PPh_3)(Me_3CCN)] (**5**)*

^{1}H NMR (CD_2Cl_2, 293 K, ppm): δ = 7.19–7.35 (m,15H, P*Ph*$_3$), 7.07 (s, 2H, IMes *m*-C*H*), 7.05 (s, 2H, IMes *m*-C*H*), 7.00 (s, 2H, IMes NC*H* = C*H*N), 2.40 (s, 6H, IMes *p*-CH_3), 2.31 (s, 6H, IMes *o*-CH_3), 2.21 (s, 6H, IMes *o*-CH_3), 1.14 (s, 9H, Me_3CN, CH_3), −20.01 (br. s, 1H, Ru-*H*). (Additionally, few peaks which could not be assigned were also noted). **^{31}P{^{1}H} NMR** (CD_2Cl_2, ppm): δ = 41.1 (s, 1P, *P*Ph$_3$). **^{13}C{^{1}H} NMR** (CH_2Cl_2; $CDCl_3$ ext. lock, ppm): δ = 201.9 (d, $^{2}J_{CP}$ cis = 12.0 Hz, *C*O), 187.6 (d, $^{2}J_{CP}$ trans = 103.0 Hz, IMes N*C*N), 138.4 (s, IMes), 137.4 (s, IMes), 136.6 (s, IMes), 136.3 (s, IMes),135.7 (d, $^{1}J_{CP}$ = 37.0 Hz, *i*-P*Ph*$_3$), 134.5 (d, $^{2}J_{CP}$ = 11.0 Hz, *o*-P*Ph*$_3$), 129.4 (s, *p*-P*Ph*$_3$), 128.9 (s, IMes), 127.7 (d, $^{3}J_{CP}$ = 9.0 Hz, *m*–P*Ph*$_3$), 126.4 (s, Me_3CCN *C*N), 123.0 (s, IMes NC*H*=*C*HN), 28.4 (s, Me_3CCN Me_3*C*), 27.9 (s, Me_3CCN *C*H_3), 21.1 (s, IMes *p*-CH_3), 18.6 (s, IMes *o*-CH_3), 18.5 (s, IMes *o*-CH_3). IR (cm^{-1}): υ (CO) 1900 (KBr).

*2.2.9. Synthesis and characterization of [RuCl(η^2-H_2)(CO)(IMes)(PPh_3)(L/L′)](OTf) (L = py, **6**; 4Mepy, **7**; L′ = MeCN, **8**; Me_3CCN, **9**)*

Complexes **2–5** [18 mg, **2**; 20 mg, **3**; 19 mg, **4**; 20 mg, **5**; (0.02–0.025 mmol)] were dissolved in 0.3 mL of CD_2Cl_2 in Schlenk NMR tubes. These solutions were subjected to two freeze–pump-thaw degassing cycles. HOTf solution (1.5–2.0 equiv. in 0.2 mL CD_2Cl_2) was added to each of the solutions of **2–5** at liq. N_2 temperature. The NMR tubes were flame-sealed under vacuum at liq. N_2 temperature and then slowly warmed up to ~193 K (liq. N_2 and Et_2O). In each case, the tube was inserted into an NMR probe, which was pre-cooled and maintained at 183 or 193 K. The dihydrogen complexes [RuCl(η^2-H_2)(CO)(IMes)(PPh_3)(L/L′)](OTf) (L = py, **6**; 4Mepy, **7**; L′ = MeCN, **8**; Me_3CCN, **9**) were characterized using NMR spectroscopy in the temperature ranges of 183–233 K.

*2.2.10. Characterization data of [RuCl(η^2H_2)(CO)(IMes)(PPh_3)(py)][OTf] (**6**)*

^{1}H NMR (CD_2Cl_2, 203 K, ppm): δ = 8.40 (d, $^{3}J_{H,H}$ = 5.4 Hz, 1H, py *o*-C*H*), 7.97 (d, $^{3}J_{H,H}$ = 5.4 Hz, 1H, py *o*-C*H*), 6.92–7.40 (m, 15H, P*Ph*$_3$; 2H, IMes NC*H* = C*H*N; 1H, py *p*-C*H*), 6.94 (t, $^{3}J_{H,H}$ = 5.4 Hz, 1H, py *m*-C*H*), 6.33 (t, $^{3}J_{H,H}$ = 5.4 Hz, 1H, py *m*-CH), 2.25 (s, 6H, IMes CH_3), 2.12 (s, 6H, IMes CH_3), 1.93 (s, 6H, IMes CH_3), −8.76 (br. s, 2H, Ru-H_2). **^{31}P{^{1}H} NMR** (CD_2Cl_2, 213 K, ppm): δ = 29.3 (s, 1P, *P*Ph$_3$).

*2.2.11. Characterization data of [RuCl(H2)(CO)(IMes)(PPh3)(4Mepy)][OTf] (**7**)*

^{1}H NMR (CD_2Cl_2; 193 K, ppm): δ = 8.18 (d, $^{3}J_{H,H}$ = 5.6 Hz, 1H, 4Mepy *o*-C*H*), 7.78 (d, $^{3}J_{H,H}$ = 5.6 Hz, 1H, 4Mepy *o*-C*H*), 6.94–7.40 (m, 21H, P*Ph*$_3$, IMes NC*H* = C*H*N, *m*-C*H*), 6.11 (d, $^{3}J_{H,H}$ = 5.6 Hz, 1H, 4Mepy *m*-C*H*), 6.57 (d, $^{3}J_{H,H}$ = 5.6 Hz, 1H, 4Mepy *m*-C*H*), 2.28 (6H, IMes *p*-CH_3), 2.14 (6H, 4Mepy *o*-CH_3), 2.08 (3H, 4Mepy, *p*-CH_3), 1.94 (6H, IMes *o*-CH_3), −8.66 (br, 2H, Ru-H_2). **^{31}P{^{1}H} NMR** (CD_2Cl_2; 193 K, ppm): δ = 29.7 (s, 1P, *P*Ph$_3$).

*2.2.12. Characterization data of [RuCl(η^2H_2)(CO)(IMes)(PPh_3)(MeCN)][OTf] (**8**)*

^{1}H NMR (CD_2Cl_2, 198 K, ppm): δ = 6.98–7.19 (m, 15H, P*Ph*$_3$, 6H, IMes NC*H* = C*H*N, *m*-CH), 2.38 (6H, IMes *p*-CH_3), 2.23 (6H, IMes *o*-CH_3), 2.11 (6H, IMes *o*-CH_3), 1.03 (s, 3H, *Me*CN) −9.12 (br. s, 2H, Ru-H_2). **^{31}P{^{1}H} NMR** (CD_2Cl_2, 198 K, ppm): δ = 28.1 (s, 1P, *P*Ph$_3$).

*2.2.13. Characterization data of [RuCl(η^2H_2)(CO)(IMes)(PPh_3)(Me_3CCN)][OTf] (**9**)*

^{1}H NMR (CD_2Cl_2, 193 K, ppm): δ −9.54 (br. s, 2H, Ru-H_2). The region of the spectrum downfield to TMS was comprised of peaks that were not well resolved. Therefore, peak assignments could not be made with certainty. **^{31}P{^{1}H} NMR** (CD_2Cl_2, 193 K, ppm): δ = 22.0 (s, 1P, *P*Ph$_3$).

*2.2.14. Synthesis of [RuHCl(CO)(PPh_3)$_2$(py)] (**10/11**)*

Addition of 1 mL of pyridine (py) to [RuHCl(CO)(PPh_3)$_3$] (220 mg, 0.23 mmol) at room temperature resulted in the formation of a greyish white precipitate in 30–40 min. Addition of excess hexane gave more quantity of precipitate. The supernatant liquid was removed completely and the precipitate was washed twice with 5 mL of hexanes. The precipitate containing the isomer products **10** and **11** was dried under vacuum and isolated in a high yield (150 mg, yield = 85%). The ^{1}H, ^{31}P{^{1}H}, and ^{13}C{^{1}H} NMR and IR spectra were recorded for characterization (Table 4). NMR spectroscopy revealed that the resultant product is a mixture of two isomers [RuHCl(CO)(PPh_3)$_2$(Py)] [**10/11**($trans_{HCl}$/cis_{HCl} = 85/15)].

*2.2.15. Characterization data of [RuHCl(CO)(PPh_3)$_2$(py)] (**10**)*

^{13}C{^{1}H} NMR ($CDCl_3$, room temperature, 100 MHz): δ = 205.4 (t, $^2J_{CP}$ 16 Hz, *C*O), 153.1–157.2 (m, py), 135.2 (s, P*Ph*$_3$), 134.0 (t, $^1J_{CP}$ = 5.9 Hz, *i*-P*Ph*$_3$), 129.3 (t, P*Ph*$_3$), 127.9 (t, $^2J_{CP}$ = 4 Hz, *o*-PPh$_3$), 122.9–123.6 (m, py). IR (cm^{-1}): ν(CO). Anal. calcd for $C_{42}H_{36}ClNOP_2Ru$ (769), C: 65.58, H: 4.72, N: 1.82. Found: C: 65.41, H: 4.59, N: 1.79.

*2.2.16. Synthesis of [RuHCl(CO)(PPh_3)$_2$(4Mepy)] (**12/13**)*

Complexes **12/13** were also prepared and isolated in a similar manner to that of complexes **10/11** using 2 mL of 4Mepy and [RuHCl(CO)(PPh_3)$_3$] (575 mg, 0.6 mmol). The resulting mixture of isomers was isolated in a high yield (~400 mg, 85%). The ^{1}H, ^{31}P{^{1}H}, and ^{13}C{^{1}H} NMR and IR spectra were recorded for characterization of **12/13**. The ^{1}H and ^{31}P{^{1}H} NMR and IR data for complexes **10–13** are given in Supplementary Material.

*2.2.17. Characterization data of [RuHCl(CO)(PPh_3)$_2$(4Mepy)] (**12**)*

^{13}C{^{1}H} NMR ($CDCl_3$, room temperature, 100 MHz): δ = 205.4 (t, $^2J_{CP}$ 16.0 Hz, *C*O), 152.5–156.7 (m, 4M*e*p*y*), 147.0 (s, P*Ph*$_3$), 134.5(t, $^1J_{CP}$ = 5.9 Hz, *i*-P*Ph*$_3$), 129 (s, P*Ph*$_3$), 127.8 (t, $^2J_{CP}$ = 4.5 Hz, *o*-P*Ph*$_3$), 124.6 (m, 4M*e*p*y*), 20.6 (4*Me*py). IR (cm^{-1}): ν(CO). Anal. calcd for $C_{43}H_{38}ClNOP_2Ru$ (783), C: 65.94, H: 4.89, N: 1.79; Found: C: 65.56, H: 4.71, N: 1.81.

*2.2.18. Synthesis of [RuCl(η^2-H_2)(CO)(PPh_3)$_2$(L)](OTf) [L = py, **14/15**; 4Mepy, **16/17**]*

[RuHCl(CO)(PPh_3)$_2$(L)] (L = py, **10/11**; 4Mepy, **12/13**) (0.02–0.025 mmol) complexes were dissolved in 0.3 mL of CD_2Cl_2 in a Schlenk NMR tube. Each solution was then subjected to two cycles of freeze–pumpthaw degassing. 3–5 equiv. of HOTf solution in 0.2 mL of CD_2Cl_2 was added to each of the solution of **10/11** or **12/13** at liq. N_2 temperature. The NMR tube was flame sealed at liq. N_2 temperature and then it was slowly warmed to ~193 K (liq. N_2 and diethylether) and inserted into an NMR probe which was pre-cooled and maintained at 193 K. The dihydrogen complexes [RuCl(η^2-H_2)(CO)(PPh_3)$_2$(L)](OTf) (L = py, **14/15**; 4Mepy, **16/17**) were characterized by NMR spectroscopy at low temperature (193–263 K).

*2.2.19. NMR data for [RuCl(H_2)(CO)(PPh_3)$_2$(py)](OTf) (**14/15**)*

14: ^{1}H NMR (CD_2Cl_2, 223 K, 400 MHz): δ = 7.88 (br s, 1H, py, *o*-C*H*), 7.71 (br s, 1H, py, *o*-C*H*), 7.33–7.47 (m, 30H, PPh_3; 1H, py, *p*-C*H*), 6.82 (s, 1H, py, *m*-C*H*), 6.48 (s, 1H, py, *m*-C*H*), −7.49 (br. s, 2H, Ru-H_2). ^{31}P{^{1}H} NMR (CD_2Cl_2, 293 K, 161 MHz): δ = 30.8 (s, 2P, *PPh*$_3$).

15: ^{1}H NMR (CD_2Cl_2, 223 K, 400 MHz): δ = 8.18 (m, 2H, py, *o*-C*H*), 7.33–7.47 (m, 30H, PPh_3; 1H, py, *p*-C*H*), 7.04 (br s, 2H, py, *m*-C*H*), −7.88 (br. s, 2H, Ru-H_2). ^{31}P{^{1}H} NMR (CD_2Cl_2, 293 K, 161 MHz): δ = 30.0 (s, 2P, *PPh*$_3$).

*2.2.20. NMR data for [RuCl(H_2)(CO)(PPh_3)$_2$(4Mepy)](OTf) (**16/17**)*

16: ^{1}H NMR (CD_2Cl_2, 223 K, 400 MHz): δ = 7.73 (d, 5.8 Hz, 1H, 4Mepy, *o*-C*H*), 7.20–7.50 (m, 30H, PPh_3; 2H, 4Mepy, *o*-C*H* *p*-C*H*), 6.62 (d, 4.4 Hz, 1H, 4Mepy, *m*-C*H*), 6.28 (d, 5.8 Hz, 1H, 4Mepy, *m*-C*H*) −7.50 (br s, 2H, Ru-H_2). ^{31}P{^{1}H} NMR (CD_2Cl_2, 293 K, 161 MHz): δ = 30.9 (s, 2P, *PPh*$_3$).

17: ^{1}H NMR (CD_2Cl_2, 223 K, 400 MHz): δ = 7.20–7.50 (m, 30H, P*Ph*$_3$), −7.82 (br s, 2H, Ru-H_2) (4MePy peaks of complex **17** were overlapped with signals of unreacted hydride precursor **12** ^{31}P{^{1}H} NMR (CD_2Cl_2, 223 K, 161 MHz): δ = 29.6 (s, 2P, *PPh*$_3$).

*2.3. X-ray crystal structure determination of complexes **2**, **3** and **12***

Pale yellow colored crystals of complexes **2**, **3**, and **12** suitable for a diffraction study were chosen and picked carefully under a microscope. The diffraction data were collected at 100 K for complexes **2** and **3** and at 293 K for complex **12**. The unit cell parameters and intensity data were collected using a BRUKER SMART APEX CCD diffractometer equipped with a fine focus Mo-K_α X-ray source. The SMART software was used for data acquisition and the SAINT program was used for data reduction. The structures were solved by direct methods using SHELX-97. The complexes **2** and **3** crystallized in the monoclinic $P2_{1/c}$ space group with four molecules in a unit cell. However, complex **12** crystallized in the monoclinic $P2_1$ space group. All the non-hydrogen atoms were refined anisotropically and the refinement was carried out against F^2 with the help of SHELX-97 [17]. The hydride hydrogen atoms were located on a difference Fourier map while all the other hydrogen atoms

Table 2
Crystallographic data of complexes **2**, **3**, and **12**.

Complexes	**2**	**3**	**12**
Empirical formula	$C_{45}H_{45}ClN_3OPRu$	$C_{46}H_{47}ClN_3OPRu$	$C_{43}H_{38}ClNOP_2Ru$
Formula weight	811.33	825.36	783.20
Temperature (K)	100(2)	100(2)	293(2)
λ(Mo Kα) [Å]	0.71073	0.71073	0.71073
Crystal system	Monoclinic	Monoclinic	Monoclinic
Space group	*P* 2$_1$/*c*	*P* 2$_1$/*c*	*P*2$_1$
a [Å]	18.2661(10)	18.8910(8)	12.249(6)
b [Å]	14.4692(7)	14.4394(6)	25.133(13)
c [Å]	15.2464(8)	15.3921(7)	12.593(7)
α [°]	90	90	90
β [°]	105.656(1)	108.495(1)	105.282(11)
γ [°]	90	90	90
V [Å^3]	3880.1(3)	3981.7(3)	3740(3)
Z, Calculated density [Mg/m^3]	4, 1.389	4, 1.377	4, 1.391
Absorption coefficient, μ (mm^{-1})	0.553	0.540	0.611
Reflections collected/unique	31,163/7615 [R_{int} = 0.0431]	80368/7813 [R_{int} = 0.0293]	26,831/14,229 [R_{int} = 0.1443]
Goodness-of-fit on F^2	1.058	1.153	0.982
Final *R* indices [I > 2σ (I)]	R_1 = 0.0322, wR_2 = 0.0783	R_1 = 0.0279, wR_2 = 0.0625	R_1 = 0.0952, wR_2 = 0.1805
R indices (all data)	R_1 = 0.0381, wR_2 = 0.0816	R_1 = 0.0330, wR_2 = 0.0673	R_1 = 0.2329, wR_2 = 0.2429

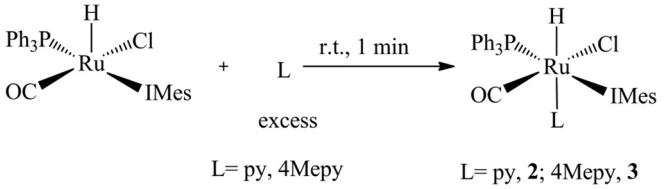

Scheme 1. Synthesis of [RuHCl(CO)(IMes)(PPh_3)(L)] (L = py, **2**; 4Mepy, **3**).

were fixed using a riding model. The crystallographic parameters are summarized in Table 2.

3. Results and discussion

3.1. Synthesis and characterization of [RuHCl(CO)(IMes)(PPh_3)(L)] (L = py, 2; 4Mepy, 3) complexes

Reaction of complex **1** with excess ligand L [L = pyridine (py) or 4-methylpyridine (4Mepy)] at room temperature afforded [RuHCl(CO)(IMes)(PPh_3)(L)] (L = py, **2**; 4Mepy, **3**) complexes in high yields (85–90%) (Scheme 1). Complexes **2** and **3** were characterized by ^{1}H, ^{31}P{^{1}H}, ^{13}C{^{1}H} NMR, and IR spectroscopy, elemental analysis, and X-ray crystallography. These complexes are stable in the solid state for about 5–6 h in air but stable for longer periods of time (> 6 months) under an inert atmosphere. Exposure of solutions of these complexes to air led to their rapid decomposition. In addition to the intractable ruthenium species, IMes.HCl and $OPPh_3$ could be identified among the decomposed products using NMR spectroscopy.

Light yellow colored crystals were obtained by slow diffusion of hexane into saturated solutions of complexes **2** and **3** in toluene at 273 K over a period of 10–12 days. The ORTEP view of complex **2** is shown in Fig. 1 and of complex **3** in Supplementary Material. The

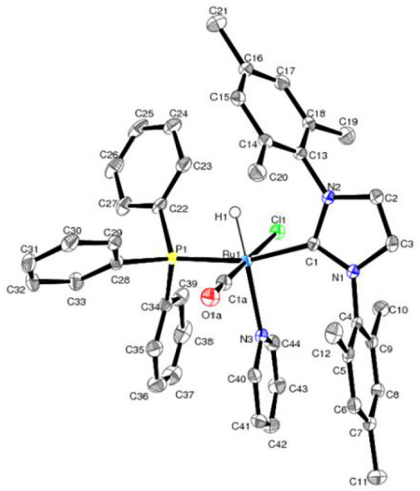

Fig. 1. ORTEP view of [RuHCl(CO)(IMes)(PPh_3)(py)] (**2**) complex.

coordination geometry around the metal center in complexes **2** and **3** could be described as a distorted octahedron. Crystal structures of both the complexes reveal that the chloride and carbonyl, hydride and py or 4Mepy, and IMes and PPh_3 are mutually *trans* to each other. A large deviation from the expected bond angle of 180° for C(1)(IMes)—Ru(1)—P(1)(PPh_3) (~165°) was noted. In both the complexes, intramolecular π-π stacking interactions involving mesityl group of IMes, pyridyl, and one of the phenyl groups of PPh_3 were observed (centroid to centroid distance: 3.5–3.6 Å) (Supplementary Material). The Ru-N bond lengths in both the complexes are comparatively longer [2.299(2) Å for complex **2** and 2.287(2) Å for complex **3**] than the previously reported pyridyl or substituted pyridyl ruthenium complexes (< 2.250 Å) [18]. The dihedral angles between Py and IMes, N1—C1—Ru1—N3 and N2—C1—Ru1—N3 in complex **2** are respectively, −13.69° and 165.04°. Similarly, the dihedral angles between 4Mepy and IMes are N1—C1—Ru1—N3 = −13.79° and N2—C1—Ru1—N3 = 165.07° in case of complex **3**, which shows that IMes and pyridyl ligands are nearly parallel to each other. Selected bond lengths and angles are summarized in Table 3.

3.2. Variable temperature (VT) NMR spectral study of [RuHCl(CO)(IMes)(PPh_3)(L)] (L = py, 2; 4Mepy, 3)

The ^{1}H NMR spectral signals of the ligands L (L = py or 4Mepy) *trans* to the hydride in complexes **2** and **3** are broad in nature at 293 K. These signals sharpen upon cooling the samples from 293 to 198 K. The ^{1}H–^{1}H COSY spectrum of complex **2** at 198 K indicates that signals of all the *ortho* and the *meta*-protons of the py ligand are distinguishable as compared to the broad features observed at 293 K. In complex **2**, five sets of aromatic proton signals were observed for the py ligand at 198 K. Similarly, four sets of aromatic proton signals were observed for 4Mepy ligand in complex **3** at 198 K. The ^{1}H NMR spectral signals of py and 4Mepy clearly suggests that the rotation around the Ru-N bond is restricted at low temperature (198 K) in both the complexes. Partial ^{1}H–^{1}H COSY spectrum and VT ^{1}H NMR spectral stack plot of complex **2** are shown in Fig. 2. VT ^{1}H and ^{31}P{^{1}H} NMR spectral stack plots of complex **3** have been deposited in the Supplementary Material. It is also clear from the crystal structures that the steric environment of both the *ortho* and the *meta*-carbon atoms of py or 4Mepy are different due to π-π stacking (Supplementary Material).

Attempts to synthesize [RuHCl(CO)(IMes)(PPh_3)(Coll)] complex (Coll = 2,4,6-collidine) were unsuccessful. The reaction did not occur even when neat ligand was used instead of a stoichiometric quantity as a solution in a solvent. This could be ascribed to the sterically bulky nature of the 2,4,6-collidine ligand.

3.3. Synthesis and characterization of [RuHCl(CO)(IMes)(PPh_3)(L′)] (L′ = MeCN, 4; Me_3CCN, 5) complexes

Initial attempts to isolate the nitrile complexes [RuHCl(CO)(IMes)(PPh_3)(L′)] (L′ = MeCN, **4**; Me_3CCN, **5**) from the reaction of complex **1** with the nitrile ligand L′ (L′ = MeCN or Me_3CCN), were unsuccessful due to the labile nature of the nitrile ligand in solution. The ligands L′

Table 3
Selected bond distances (Å) and bond angles (°) of complexes **2** and **3**.

Bond distances (Å)	(2)	(3)	Bond angles (°)	(2)	(3)
Ru(1)—C(1)	2.109(2)	2.104(2)	C(1)—Ru(1)—P(1)	165.2(1)	164.7(1)
Ru(1)—C(1A)	1.801(6)	1.798(5)	C(1)—Ru(1)—N(3)	100.5(1)	101.3(1)
Ru(1)—Cl(1)	2.480(1)	2.483(2)	P(1)—Ru(1)—N(3)	93.1(1)	93.1(1)
Ru(1)—P(1)	2.336(1)	2.338(1)	N(3)—Ru(1)—H(1)	178.1(11)	175.8(9)
Ru(1)—H(1)	1.470(3)	1.540(2)	C(1A)—Ru(1)—Cl(1)	178.0(2)	178.1(1)
Ru(1)—N(3)	2.299(2)	2.287(2)	C(1A)—Ru(1)—C(1)	89.9(15)	89.7(1)
C(1A)—O(1A)	1.170(8)	1.175(4)	P(1)—Ru(1)—Cl(1)	86.5(1)	86.6(1)
			P(1)—Ru(1)—H(1)	85.1(10)	82.9(9)

Table 4
Numbering scheme for the complexes.

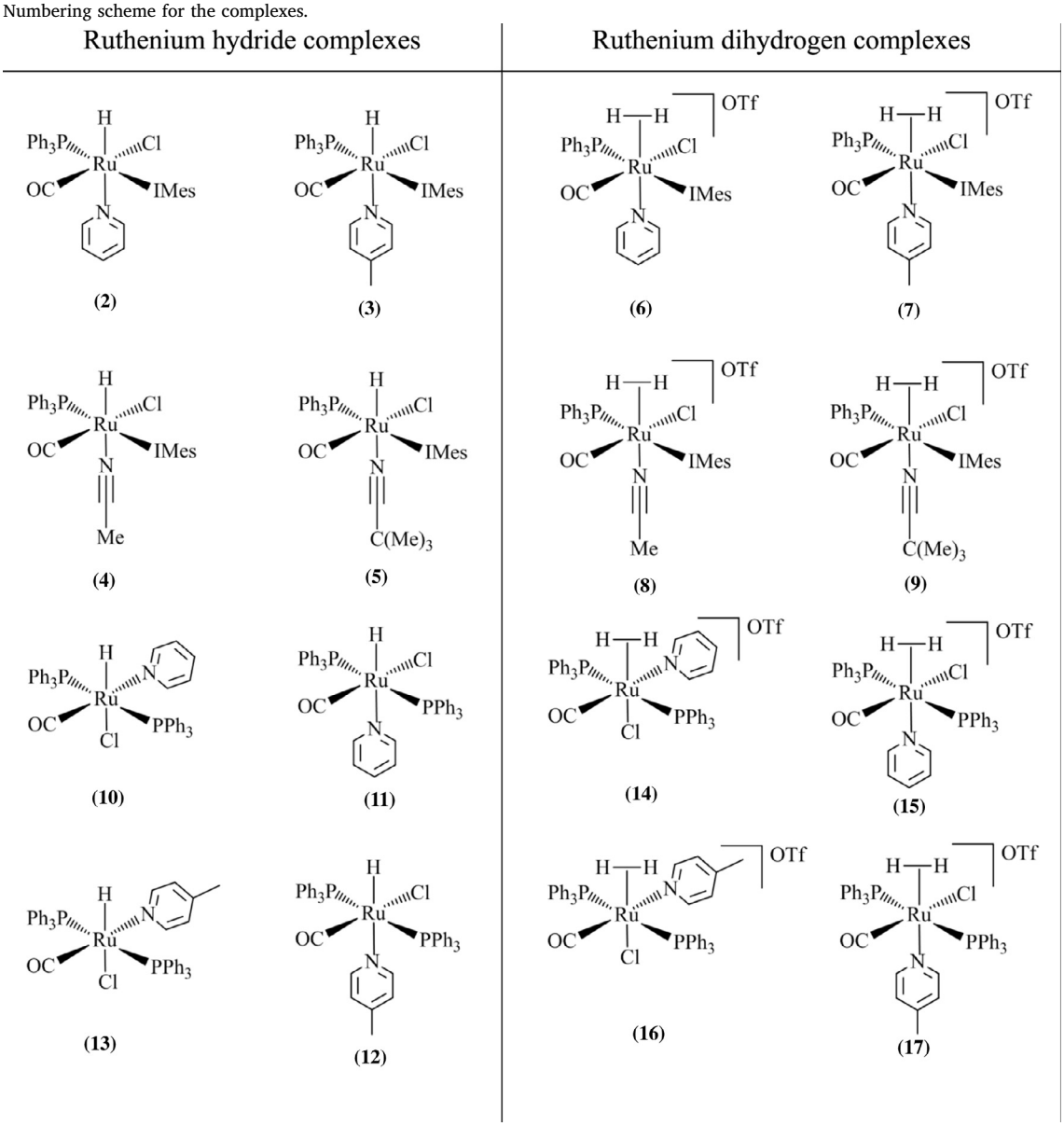

could be easily removed under vacuum with concomitant recovery of complex **1**. Initially, the reaction of complex **1** with L′ (L′ = MeCN or Me_3CCN) was monitored by ^1H and $^{31}P\{^1H\}$ NMR spectroscopy in the solution state without attempting isolation of products (Supplementary Material).

In the ^1H NMR spectra of **4** and **5**, a variation in the chemical shift of the hydride and methyl moieties of the ligand (MeCN or Me_3CCN) was noted as the concentration of the free ligand (MeCN or Me_3CCN) was varied. When excess nitrile was used, a new doublet for the hydride ligand at δ −13.35 ppm (d, $^2J_{PH}$ = 19.4 Hz in case of MeCN ligand) and at δ −13.45 ppm (d, $^2J_{PH}$ = 18.3 Hz in case of Me_3CCN ligand) were also observed along with signals of **4** and **5** (Supplementary Material). Esteruelas and co-workers reported that the reaction of $[Os(H)_2(Cl)_2(P^iPr_3)_2]$ with MeCN lead to the formation of $[Os(Cl)_2(\eta^2\text{-}H_2)(MeCN)(P^iPr_3)_2]$ and $[OsCl(\eta^2\text{-}H_2)(MeCN)_2(P^iPr_3)_2]Cl$ complexes. The formation of $[OsCl(\eta^2\text{-}H_2)(MeCN)_2(P^iPr_3)_2](Cl)$ was due to the displacement of one of the chloride ligands of $[Os(Cl)_2(\eta^2\text{-}H_2)(MeCN)(P^iPr_3)_2]$ by MeCN [18d]. Similarly, in the present work, new hydride complexes $[RuH(CO)(IMes)(PPh_3)(L')_2]Cl$ (L′ = MeCN, **4a**; Me_3CCN, **5a**) were obtained by the displacement of the Cl ligand in **4** and **5** by MeCN or Me_3CCN ligands, respectively. A partial ^1H NMR spectral stack plots of Ru-H and methyl protons of ligand L′ (L′ = MeCN, **4**; Me_3CCN, **5**) upon addition of different quantities of L′ have been deposited in the Supplementary Material.

In solution, the nitrile ligands in these complexes were found to be labile. The ligands L′ could be easily removed under vacuum with concomitant recovery of complex **1**, which made their isolation difficult. However, in the solid state, these ligands are tightly bound to the metal center. Considering these observations, attempts were made to isolate complexes **4** and **5** by carrying out the reactions in neat MeCN or Me_3CCN which led to the precipitation of these complexes. Thus, complexes **4** and **5** were isolated in the solid state in this manner (Scheme 2). The isolated products were characterized by ^1H, $^{31}P\{^1H\}$, and $^{13}C\{^1H\}$ NMR and IR spectroscopy. The ^1H NMR spectrum is comprised of a broad singlet for the hydride hydrogen at δ −15.97 and −20.01 ppm for complexes **4** and **5**, respectively. The $^{13}C\{^1H\}$ NMR spectrum showed a doublet for CO at *δ* 203.0 ppm ($^2J_{P,C}$ *cis*: 13.5 Hz; Ru-*C*O, **4**), 201.9 ppm ($^2J_{P,C}$ *cis*: 13.5 Hz; Ru-*C*O, **5**), and a doublet for

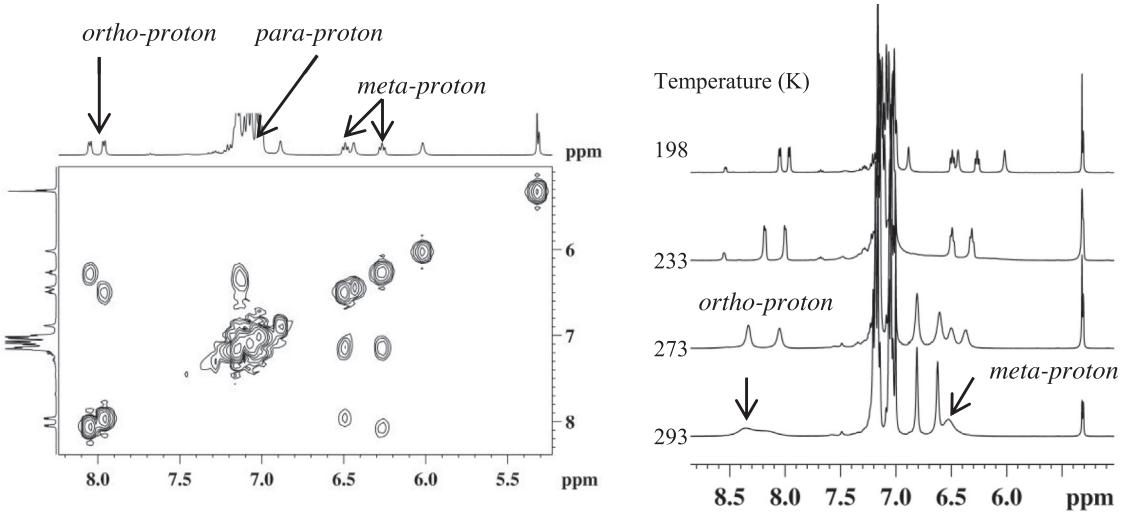

Fig. 2. Partial $^{1}H–^{1}H$ COSY NMR spectrum at 198 K (left) and VT ^{1}H NMR spectral stack plot (right) of complex **2**.

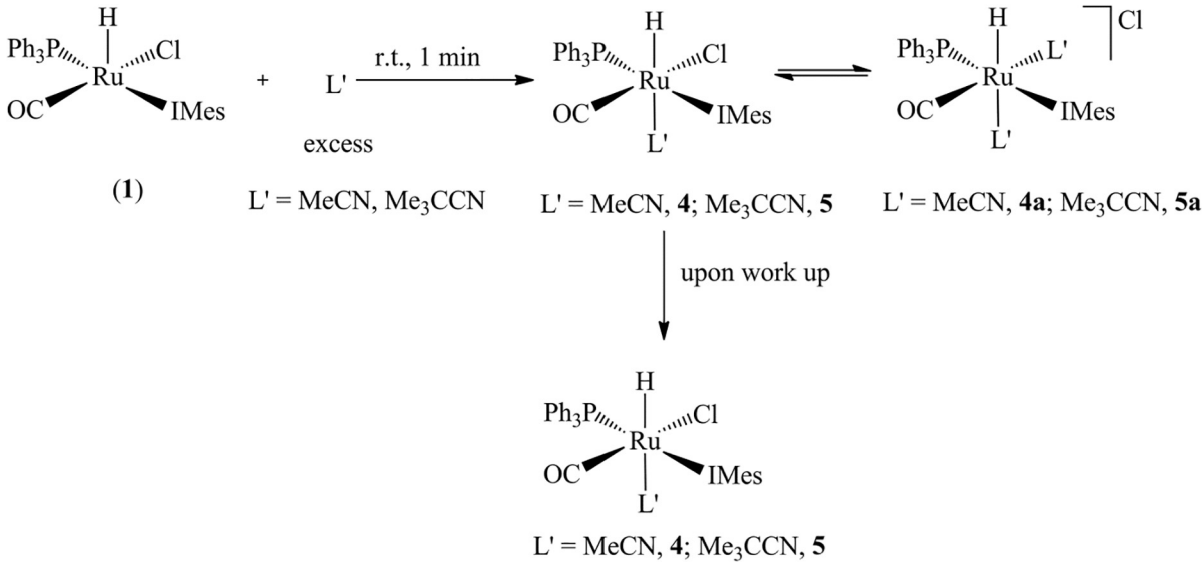

Scheme 2. Synthesis of complexes **4** and **5**.

carbene carbon at δ 186.9 ppm ($^{2}J_{P,C}$ *trans*:102.5 Hz, Ru-N*C*N, **4**), 187.5 ppm ($^{2}J_{P,C}$ *trans*:104.0 Hz, Ru-N*C*N, **5**). These values are consistent with retention of ligand environment around the ruthenium metal center. Selected spectral data of all the complexes have been given in Supplementary Material. Attempts to crystallize these complexes by slow evaporation in THF afforded only colorless crystals of IMes.HCl salt (Supplementary Material). X-ray structure determination of IMes.HCl revealed that it is a different polymorph form than that reported in the literature earlier (Supplementary Material) [19].

3.4. Variable temperature (VT) NMR spectral study of [RuHCl(CO)(IMes)(PPh$_3$)(L′)] (L′ = MeCN, 4; Me$_3$CCN, 5)

An unusually large temperature-dependent chemical shifts were observed for the Ru-*H* and *methyl* protons of L′ (L′ = MeCN and Me_3CCN) in complexes **4** and **5**. In the ^{1}H NMR spectrum of complex **4**, the Ru-*H* signal appeared as a broad singlet at δ −15.97 ppm in CD_2Cl_2 at 293 K. A substantial downfield shift ($\Delta\delta$ = 3.39 ppm) from δ −15.95 (br. s, 293 K) to −12.58 ppm (d, $^{2}J_{PH}$ = 20.0 Hz,) was noted for the hydride moiety at 198 K. An upfield shift for methyl signal of MeCN from δ 1.42 (s, 293 K) to 1.11 ppm (s, 198 K) was also noted. A partial VT NMR spectral stack plot of **4** is shown in Fig. 3.

A systematic study was carried out to unravel the concentration and temperature-dependent behavior of chemical shifts of Ru-H and L′ (L′ = MeCN or Me_3CCN) for both the complexes **4** and **5** (see Supplementary Material). This study also gives an indication of the existence of an equilibrium between complexes **1** and **4** or **5**: complex **1** at room temperature due to labile nature of L′ (L′ = MeCN, Me_3CCN) and complexes **4** or **5** at low temperature due to binding of L′. Selected NMR spectral data (at 293 K and 198 K) and IR carbonyl frequency data (at room temperature) of all the complexes have been summarized in Table S10 (Supplementary Material).

3.5. Equilibrium between complexes 1 and 4 or 5 in solution

Variable temperature NMR spectral study of complexes **4** and **5** was carried out in tol-d_8 in the temperature range of 363–193 K for **4** and 343–203 K for **5**. In case of complex **4**, at 363 K, the Ru−H signal appeared at −23.37 ppm (d, $^{2}J_{H,P}$ = 24.2 Hz) which is comparable to the chemical shift of Ru−H of complex **1** (−23.89 ppm, d, $^{2}J_{H,P}$ = 24.3 Hz).

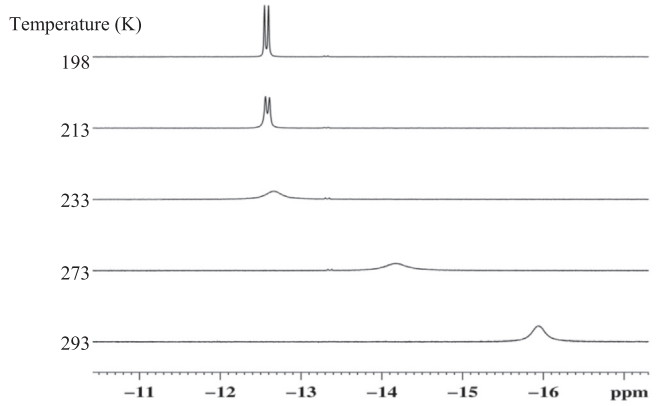

Fig. 3. VT partial ^{1}H NMR spectral stack plot for Ru-—*H* of [RuHCl(CO)(IMes)(PPh_3)(MeCN)] (**4**) in CD_2Cl_2.

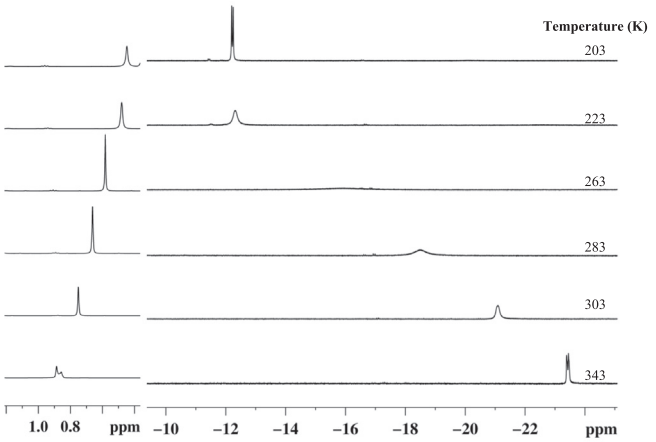

Fig. 4. VT Partial ^{1}H NMR spectral stack plot of [RuHCl(CO)(IMes)(PPh_3)(Me_3CCN)] (**5**) in tol-d_8.

Upon cooling a sample of complex **4**, the ^{1}H NMR spectral signal of Ru-H merged with the baseline at 243 K and then reappeared at a temperature < 243 K; at 193 K, this signal re-appeared as a doublet at −11.88 ppm (d, $^{2}J_{H,P}$ = 20.5 Hz). Similarly, the signal due to the methyl group of MeCN ligand underwent an upfield shift of 0.49 ppm (from 0.85 ppm at 363 K to 0.36 ppm at 193 K) (Supplementary Material).

These observations indicate the existence of an equilibrium between complexes **1** and **4**; at high temperature, the equilibrium is shifted to the left and at low temperature, it is shifted to the right (Scheme 3). Thermodynamic parameters were obtained for complex **4** using the VT NMR spectral data. The ΔH and ΔS values were calculated from a plot of $R\ln K_{eq}$ versus 1/T and found to be −5.75 kcalmol^{-1} and −20.79 cal mol^{-1} K^{-1}, respectively.

Similarly, in case of complex **5**, at 343 K, the Ru-H signal appeared at −23.43 ppm (d, $^{2}J_{H,P}$ = 24.1 Hz) which is comparable to the chemical shift of Ru—H of complex **1** (−23.89 ppm, d, $^{2}J_{H,P}$ = 24.3 Hz). Upon cooling the sample of complex **5**, the ^{1}H NMR spectral signal of Ru—H merged with the baseline at 263 K and then reappeared as a doublet at −12.22 ppm (d, $^{2}J_{H,P}$ = 20.0 Hz) at 193 K. Similarly, the signal due to the methyl group of Me_3CCN ligand underwent an upfield shift of 0.42 ppm from 0.87 ppm at 343 K to 0.45 ppm at 193 K. All temperature-dependent chemical shifts of Ru-*H* moiety and MeCN and Me_3CCN ligands of complexes **4** and **5** have been plotted and deposited in the Supplementary Material. A variable temperature NMR spectral stack plot of complex **5** is shown in Fig. 4. These observations are also indicative of an equilibrium between complexes **1** and **5** (Scheme 3). The thermodynamic parameters, in this case, were also calculated and deposited in the Supplementary Material.

The negative sign of entropy and enthalpy suggest that the reaction is feasible at low temperature. The ΔG values for both the reactions were calculated to be 0.34 kcal/mol and 0.35 kcal/mol for complexes **4** and **5**, respectively at 293 K and −1.53 kcal/mol and −1.96 kcal/mol for complexes **4** and **5**, respectively at 203 K. Details of the calculations of thermodynamic parameters of these reactions have been summarized in Supplementary Material.

VT NMR spectral study was carried out for the mixture of complexes **1** and **5** (~1:1) in CD_2Cl_2. In the ^{1}H NMR spectrum, an average broad singlet at δ −22.0 ppm was noted for Ru-H at 293 K instead of the two separate signals for both the complexes (Fig. 5). However, at 208 K, two separate doublets corresponding to Ru-H of complexes **1** and **5** appeared (Supplementary Material). The 2D-EXSY spectrum also confirmed that both the hydride signals are related via exchange of the Me_3CCN ligand. A correlation between both the Ru-H signals was observed as cross peaks (Fig. 5).

*3.6. Lability of trans ligands in [RuHCl(CO)(IMes)(PPh_3)(L)] (L = py, **2**; 4Mepy, **3**; MeCN, **4**; Me_3CCN, **5**)*

As discussed earlier, the trans nitrile ligands in complexes **4** and **5** are labile; under vacuum complex **1** could be recovered as established using NMR spectroscopy. However, ligands L (L = py and 4Mepy) were bound tightly in complexes **2** and **3** even under vacuum. On the other hand, addition of any excess Lewis base to complexes **2–5** led to the displacement of the ligand L/L′ (L = py, 4Mepy; L′ = MeCN, Me_3CCN) trans to the hydride. For example, rapid displacement of MeCN or Me_3CCN (**4** or **5**) was noted upon addition of excess py or 4Mepy to these complexes. In comparison, displacement of py or 4Mepy (**2** or **3**) by MeCN or Me_3CCN was found to be slower. These observations indicate that ligands MeCN and Me_3CCN (complexes **4** and **5**) are highly labile compared to py or 4Mepy (complexes **2** and **3**). Based on these experiments, it was found that the order of lability of the ligands in complexes **2–5** is Me_3CCN > MeCN > py ~ 4Mepy. This could be attributed to steric and electronic effects. The greater lability of Me_3CCN could be ascribed to the high steric encumbrance that it experiences in the sixth coordination site of the metal center in complex **5**. In complexes **2** and **3**, intramolecular π-πstacking interactions which are evident from the crystal structure stabilize the py and 4Mepy ligands and

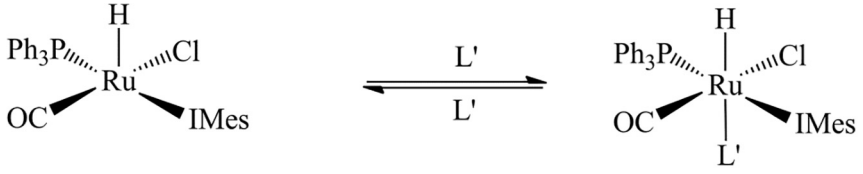

(1) L' = MeCN, Me_3CCN L' = MeCN, **4**; Me_3CCN, **5**

Scheme 3. Equilibrium between complex **1** and **4** or **5**.

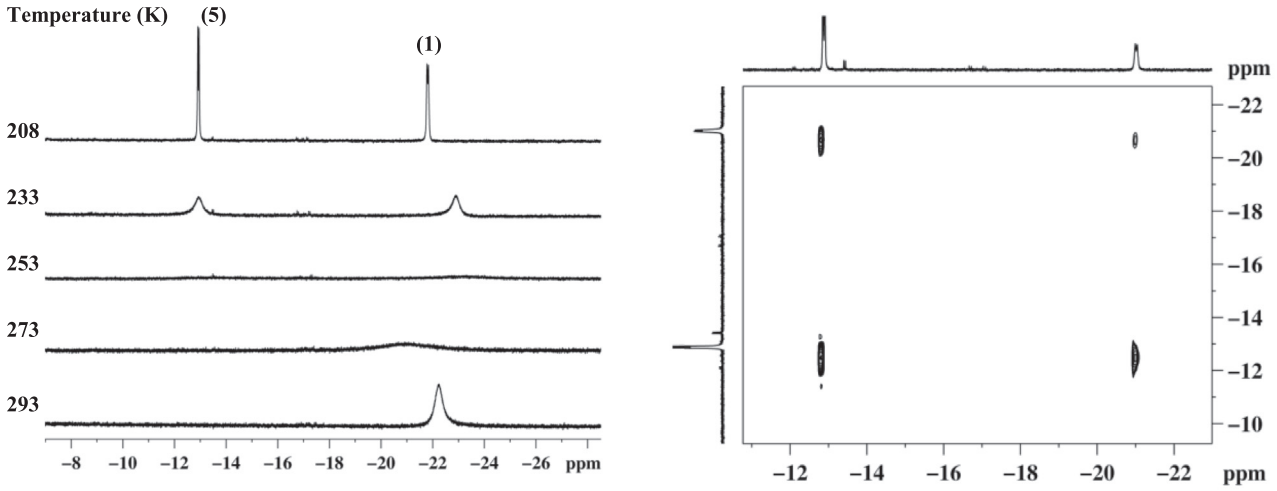

Fig. 5. 2 VT partial ^{1}H NMR spectra for Ru−H signal of **1** and **5** (left) and 2D-EXSY NMR spectrum of the Ru-H region of complexes **1** and **5** in CD_2Cl_2 at 208 K (right).

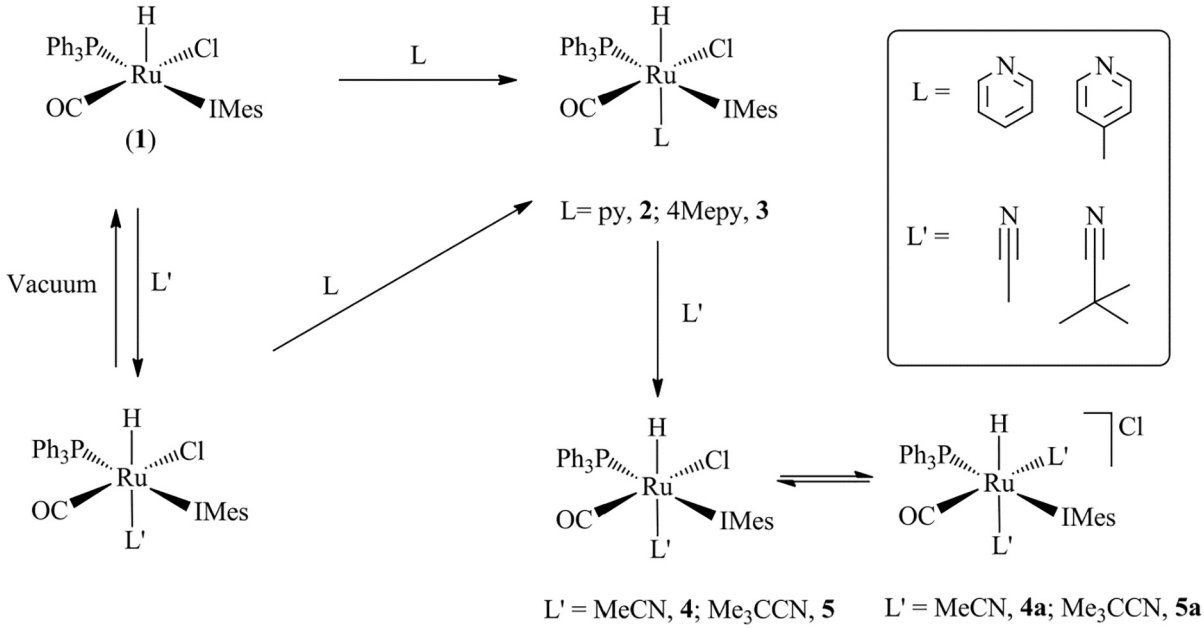

Scheme 4. Lability of *trans* ligands in complexes **2–5.**

hence provide better stability to these complexes. The possibility of π-π stacking interactions in the solution state could not be ascertained since the ^{1}H NMR spectral signals of py and 4Mepy ligands at 293 K in complexes **2** and **3** are broad. The broad nature of the signals could be attributed to the rotation of these ligands around the Ru-N bond. The bulky IMes ligand in complexes **2–5** imposes great steric crowding around the ruthenium center. In addition to the steric factor, the electronic effect of *trans* ligands is also crucial for their binding. Pyridyl ligands are better donors as compared to nitrile ligands, which could make the nitrile ligands more labile as compared to pyridyl ligands in this case. Solid and cone angles of Py (solid angle:1.90° and cone angle: 91.6°) and MeCN (solid angle: 1.60° and cone angle: 83.69°) suggest greater steric hindrance in case of Py as compared to MeCN as a ligand [20]. However, stronger binding of pyridyl ligand to the metal center in comparison to nitrile ligands could be ascribed to its better donor ability and intramolecular π-π stacking. The lability studies of complexes **2–5** is shown schematically in Scheme 4.

Peterson and co-workers reported a similar five-coordinate complex [RuHClCO(IMes)$_2$] which does not react with MeCN or PMe_3 ligand due to the presence of two sterically demanding IMes groups [21]. In comparison, complex **1** is less sterically crowded than [RuHClCO (IMes)$_2$] [21]. Thus, complex **1** reacts with MeCN and PMe_3 (Schemes 4 and 5). However, the ruthenium center in complex **4** experiences enough steric crowding that makes the MeCN ligand labile.

Addition of excess PMe_3 to solutions of **2–5** in $CDCl_3$ resulted in the formation of [RuHCl(CO)(IMes)(PPh_3)(PMe_3)] via elimination of *trans* ligands (py, 4Mepy, MeCN, Me_3CCN), which further confirm the labile nature of *trans* ligands. Upon elimination of labile ligands, [RuHCl(CO) (IMes)(PPh_3)(PMe_3)] complex transforms to [RuHCl(CO)(IMes) (PMe_3)$_2$] and [RuH(CO)(IMes)(PMe_3)$_3$](Cl) via substitution of PPh_3 and chloride ligands with another two PMe_3 ligands. The reaction proceeded similarly to the one as reported earlier by us and shown in Scheme 5 [14].

3.7. Synthesis and characterization of dihydrogen complexes bearing an NHC ligand

Protonation of the complexes **2–5** using 1.5–2.0 equiv. of HOTf at room temperature did not show any evidence for the formation of the corresponding dihydrogen complexes using NMR spectroscopy. Signals

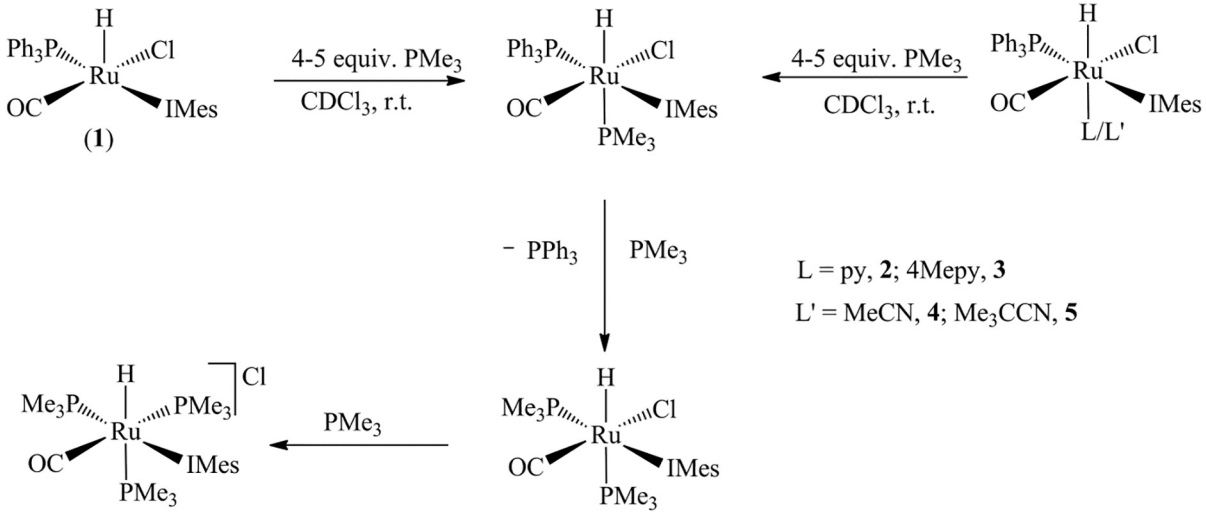

Scheme 5. Reaction of complexes **1–5** with PMe_3.

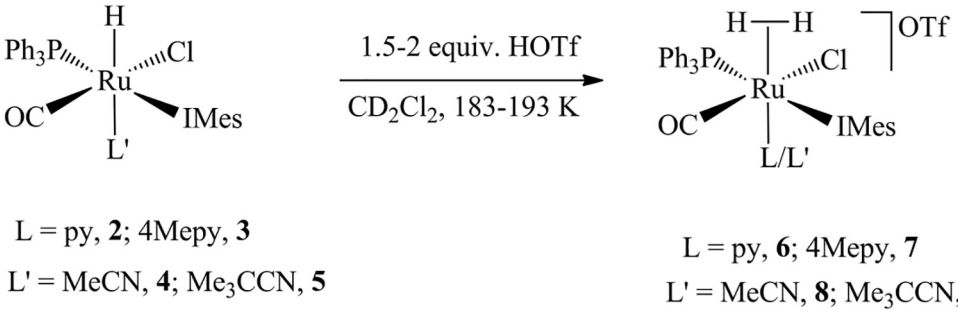

Scheme 6. Synthesis of [RuCl(η^2-H_2)(CO)(IMes)(PPh_3)(L)][OTf] complexes (L = py, **6**; 4Mepy, **7**; MeCN, **8**; Me_3CCN, **9**).

for the imidazolium salt (IMes.HOTf) and free H_2 (s, δ 4.59 ppm) were noted in the ^1H NMR spectrum. This observation indicates that the dihydrogen complexes, if formed, are unstable at room temperature. Therefore, protonation reactions of hydride complexes (**2–5**) were carried out using HOTf (1.5–2.0 equiv.) at low temperature (183–193 K) (Scheme 6). In this case, we obtained the dihydrogen complexes [RuCl(η^2-H_2)(CO)(IMes)(PPh_3)(L)]OTf (L = Py, **6**; 4Mepy, **7**; MeCN, **8**; Me_3CCN, **9**) **6–9** which were found to be stable in the temperature range of 183–233 K. Upon warming beyond 233 K, they decomposed via elimination of H_2. In addition, protonation of complex **4** was also carried out in presence of excess ligand (MeCN). We noted that the dihydrogen complex **8** was stable up to 253 K in the presence of excess ligand. The ^1H NMR spectra of complexes **6–9** are comprised of a broad singlet in the range of −8.66 to −9.55 ppm for the η^2-H_2 ligand. The intact nature of the H–H bond in these derivatives was established by measurement of VT ^1H spin-lattice relaxation time (T_1, ms, 400 MHz) and $^1J_{HD}$ in the corresponding η^2-HD isotopomers. Although we did not obtain T_1 minima, it is apparent that the short T_1 values (Supplementary Material) indicate the intact nature of the H—H bond in these complexes..

The HD isotopomers [RuCl(η^2-HD)(CO)(IMes)(PPh_3)(L)][OTf] (L = py, **6-*d***; 4Mepy, **7-*d***; MeCN, **8-*d***; Me_3CCN, **9-*d***) were synthesized similar to **6–9** using DOTf instead of HOTf. The $^1H\{^{31}P\}$ NMR spectra show 1:1:1 triplets upon nullification of the residual signal of η^2–H_2 moiety in the corresponding dihydrogen complexes using the inversion recovery pulse [22]. Complex **7-*d*** showed a 1:1:1 triplet at δ −8.72 ppm due to an η^2-HD ligand (Fig. 6).

In the present study, a small variation in $^1J_{HD}$ coupling constant for the η^2-HD isotopomers was noted as a function of temperature. The $^1J_{HD}$ values increased with increase in the temperature (Supplementary Material). Temperature-dependent $^1J_{HD}$ coupling constants of dihydrogen complexes have previously been reported in the literature [5e,23]. This type of behavior of $^1J_{HD}$ was primarily noted for elongated dihydrogen (d_{HH} = 1.0–1.3 Å) and compressed dihydride complexes (d_{HH} = 1.3–1.6 Å). However, this behavior is rather unusual in case of true dihydrogen (d_{HH} = < 1.0 Å) or dihydride complexes (d_{HH} = > 1.6 Å). In the literature, temperature-dependence of $^1J_{HD}$ in elongated dihydrogen complexes has been rationalized by taking into consideration, the temperature-dependence characteristic of the H-H distance [23]. For example, Heinekey and co-workers reported temperature-dependent $^1J_{HD}$ values for [IrCp*(dmpm)H_2][$B(C_6F_5)_4$]$_2$ (dmpm = bis(dimethylphosphino)methane) (9.0 Hz at 303 K; 7.3 Hz at 223 K) [23a]. This type of behavior was ascribed to the temperature-dependent equilibrium between the two isomeric species: dihydrogen and dihydride. Mort and Autschbach further supported this observation using theoretical calculations [23c]. Similarly, an osmium dihydrogen complex reported by Maltby *et al.*, [Os(dppe)$_2$Cl(H_2)](PF_6) (dppe = $Ph_2PCH_2CH_2PPh_2$) in which $^1J_{HD}$ value increases with an increase in sample temperature (13.6 Hz at 253 K; 14.2 Hz at 308 K) [5e].

In the present work, we noted that the $^1J_{HD}$ value increases from 27.3 to 30.3 Hz upon raising the temperature of the sample from 183 to 233 K (Supplementary Material). This behavior could be rationalized by considering the lability of the *trans* ligands. It was observed that the *trans* ligand binds to the metal center strongly at low temperature (183–193 K) and is either weakly bound or labile at high temperature (233 K). As a result, the H—H bond distance in dihydrogen complexes **6–9** is dependent on the temperature. The H—H distances (d_{HH}, Å) were calculated from the measurement of $^1J_{HD}$ of the HD isotopomer of all the complexes [6a]. Similar trends were noted in the variation of the H—H distance with temperature for the complexes **6–8**. The variation in the pattern in case of complex **9** could be ascribed to the poor binding of the H_2 ligand to the metal center as compared to the other *trans*

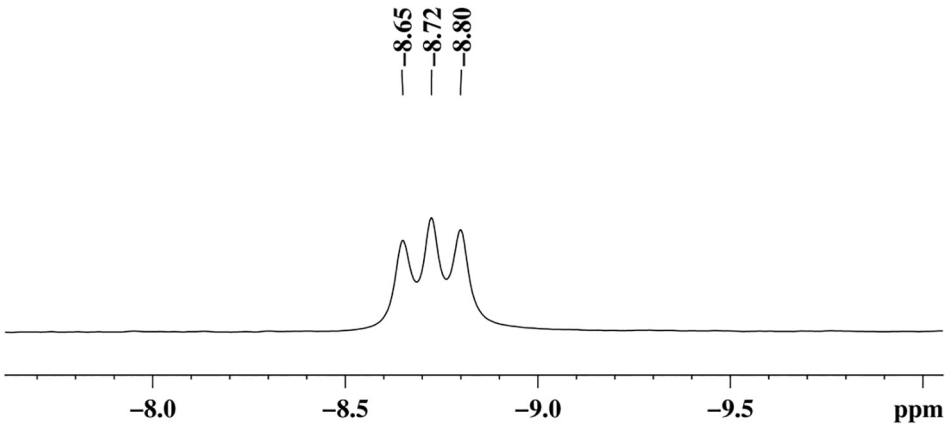

Fig. 6. Partial ^{1}H NMR spectrum of [RuCl(η^2-*HD*)(CO)(IMes)(PPh_3)(4Mepy)][OTf] (**7-*d***) in CD_2Cl_2 at 233 K.

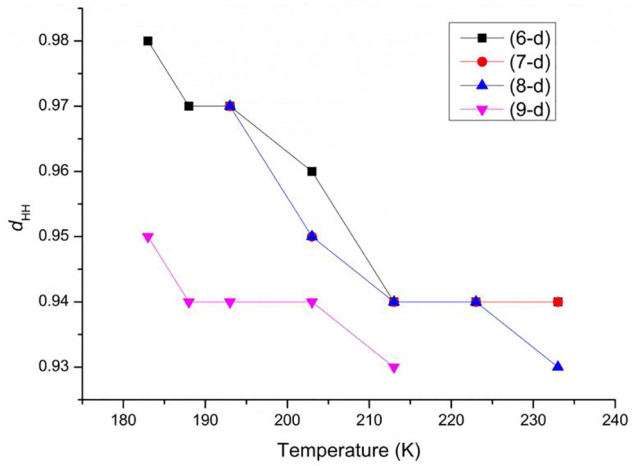

Fig. 7. Temperature versus d_{HH} (Å) plot for **6-*d*, 7-*d*, 8-*d*** and **9-*d***.

ligands, which results in a decrease in the H−H distance.

The H-H distance (d_{HH}) in complexes **6–9** were found to be 0.98–0.93 Å in the temperature range of 183–233 K (Fig. 7) [6a]. Thus, complexes **6–9** are examples of true dihydrogen complexes. Temperature dependence of the H-H distance in these dihydrogen complexes is a manifestation of the lability of the *trans* ligands.

With a view to establish that the variation of d_{HH} is a manifestation of the lability of trans ligands, we attempted to synthesize the phosphine analogues of complexes **6–7** and measure the H-H distances in them.

3.8. Synthesis and characterization of phosphine complexes

Attempts were made to prepare phosphine analogues of [RuHCl(CO)(IMes)(PPh_3)(L)] (L = py, **2**; 4Mepy, **3**) of the type [RuHCl(CO)(PPh_3)$_2$(L)] (py and 4Mepy). Malecki and co-workers reported that refluxing a mixture of [RuHCl(CO)(PPh_3)$_3$] and py in methanol affords [RuHCl(CO)(PPh_3)$_2$(py)] (*trans*$_{HCl}$) (**10**) [18a]. Herein, attempts were made to prepare and isolate its *cis*-isomer [RuHCl(CO)(PPh_3)$_2$(py)] (*cis*$_{HCl}$) (**11**); the *cis*-isomer has structural similarity to complex **2**.

Reaction of [RuHCl(CO)(PPh_3)$_3$] in neat py or 4Mepy gave a mixture of *cis* and *trans* isomers [RuHCl(CO)(PPh_3)$_2$(L)] [(L) = py, **10/11** (*trans*$_{HCl}$/*cis*$_{HCl}$); 4Mepy, **12/13** (*trans*$_{HCl}$/*cis*$_{HCl}$)] complexes at room temperature (Scheme 7). Structures of the complexes **10–13** were established by NMR and IR spectroscopy (Supplementary Material). Complex **12** was also structurally characterized using X-ray

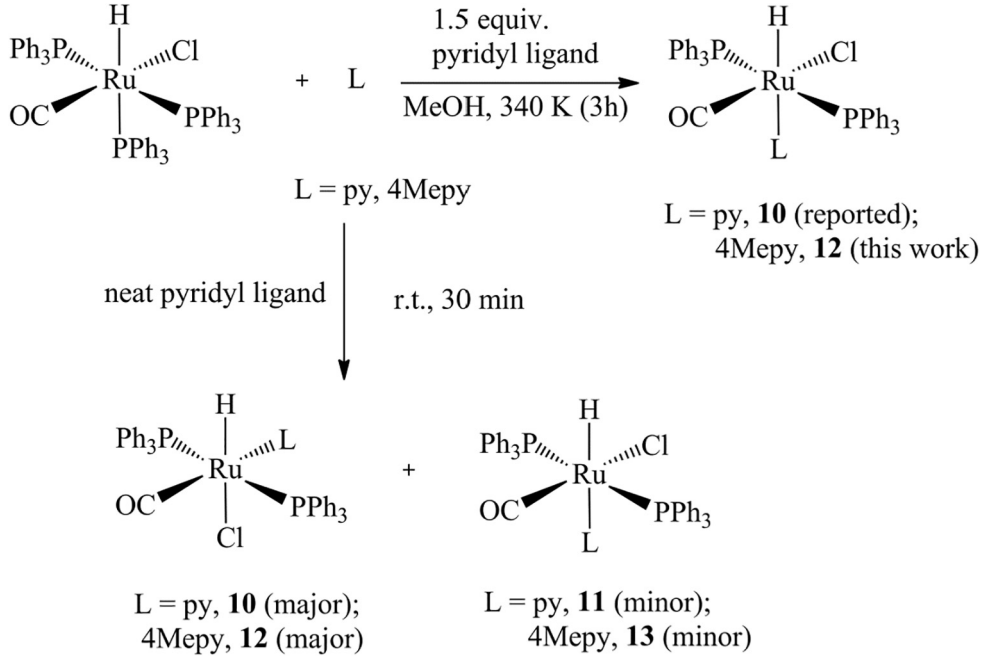

Scheme 7. Synthesis of ruthenium hydride complexes bearing phosphine ligands.

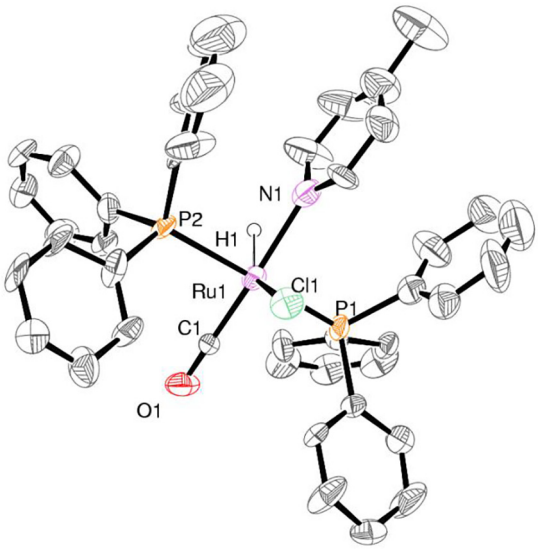

Fig. 8. ORTEP view of [RuHCl(CO)$(PPh_3)_2$(4Mepy)] (**12**).

crystallography. In the ^{1}H NMR spectrum of the isomeric complex mixture **10/11**, the hydride hydrogen appears at δ −13.27 ppm (t, $^2J_{H,P}$ = 19.0 Hz; **10,** major) and −12.49 ppm (t, $^2J_{H,P}$ = 18.0 Hz; **11**, minor). The ^{31}P{^{1}H} NMR spectrum shows two singlets at δ 46.1 (**10**, major) and 44.1 ppm (**11**, minor). In the ^{1}H NMR spectrum of **12/13**, two triplets at −13.28 ppm (t, $^2J_{H,P}$ = 19.0 Hz; **12**, major) and −12.48 ppm (t, $^2J_{H,P}$ = 19.0 Hz; **13**, minor) were noted for the Ru-*H* ligand (Supplementary Material). The ^{31}P{^{1}H} NMR spectrum showed two singlets at δ 46.0 (**12**, major) and 43.9 ppm (**13**, minor). The ^{13}C{^{1}H} NMR spectrum showed a triplet at δ 205.4 ppm for the CO ligand due to coupling ($^2J_{C,P}$ = 16.0 Hz) with two *cis* phosphorus atoms for complex **12**. However, due to the small amount of complex **13** present in solution, the signal for its CO ligand could not be detected in the ^{13}C{^{1}H} NMR spectrum. The IR stretching frequencies for CO ligands in **10–13** were noted at 1938 cm^{-1}, **10**; 1917 cm^{-1}, **11**; 1907 cm^{-1}, **12**; 1890 cm^{-1}, **13**; these are greater than those of IMes analogues (1877 cm^{-1}, **2**; 1874 cm^{-1}, **3**) which is consistent with the stronger σ donor ability of IMes over the PPh_3 ligand.

Yellow colored crystals of complex **12** were obtained via slow evaporation of solvent from a saturated solution of **12** in methanol at room temperature [18a]. The structure was established by X-ray crystallography. ORTEP view of complex **12** is shown in Fig. 8. The coordination geometry around the metal center could be described as a distorted octahedron. Crystal structure of complex **12** reveals that

Table 5
$^1J_{HD}$ (Hz) and d_{HH} (Å) data of **14-*d*, 15-*d*, 16-*d***, and **17-*d***.

Temp (K)	**14-*d***		**15-*d***		**16-*d***		**17-*d***	
	$^1J_{HD}$	d_{HH}	$^1J_{HD}$	d_{HH}	$^1J_{HD}$	d_{HH}	$^1J_{HD}$	d_{HH}
213	28.5	0.96	30.0	0.93	28.5	0.96	30.4	0.93
223	28.8	0.96	30.3	0.93	28.8	0.96	30.5	0.93
233	29.3	0.95	30.5	0.93	29.2	0.95	30.6	0.93
243	29.3	0.95	30.6	0.93	29.4	0.95	30.5	0.93
253	29.3	0.95	30.6	0.93	29.4	0.95	30.6	0.93
263	29.3	0.95	–	–	29.4	0.95	–	–

Experimental error for $^1J_{HD}$ is ± 0.2 to ± 0.4 Hz.

4Mepy and CO, hydride and chloride, and both PPh_3 ligands are mutually *trans* to each other. Ru—N bond length in complex **12** is comparatively shorter [2.187(17) Å] than the Ru—N bond length in [RuHCl(CO)(IMes)(PPh_3)(L)] complexes (L = py, **2**; 4Mepy, **3**) [Ru—N = 2.299 (2) Å, **2**; 2.287(2)]. However, this bond length is comparable to the previously reported ruthenium pyridyl complexes reported in the literature [18a,18b]. Crystallographic details are given in Table 2.

3.9. Synthesis of ruthenium dihydrogen complexes bearing phosphine ligands

Synthesis of [RuCl(η^2-H_2)(CO)$(PPh_3)_2$(L)]OTf [L = py, **14/15**, ($trans_{HCl}$/cis_{HCl}); 4Mepy, **16/17**, ($trans_{HCl}$/cis_{HCl}) was carried out similar to that of **6–9** at low temperature (193 K), since these dihydrogen complexes are also unstable at room temperature (Scheme 8). The VT spin-lattice relaxation time (T_1, 400 MHz, Supplementary Material) and $^1J_{HD}$ values (Table 5) of the HD isotopomers [RuCl(η^2-HD)(CO)$(PPh_3)_2$(4Mepy)]OTf (**16-*d*/17-*d*,** major/minor) indicate the intact nature of the H—H bond in these complexes. ^{1}H{^{31}P} NMR spectra of HD isotopomers of **16-*d*/17-*d*** are comprised of two triplets with intensity ratios of 1:1:1 (Fig. 9).

From Table 5, it is apparent that the H-H distances (0.95–0.96 Å) are invariant with a change in temperature as in complexes **14** and **16** and 0.93 Å in complexes **15** and **17**. Since chloride is a stronger σ donor compared to py or 4Mepy, the H-H distance in complexes **14** and **16** are slightly longer (0.95–0.96 Å) than in **15** and **17** (0.93 Å).Whereas, complexes [RuCl(η^2-H_2)(CO)(IMes)(PPh_3)(L)][OTf] (L = py, **6**; 4Mepy, **7**) which are analogous to complexes **15** and **17**, show temperature-dependent H—H bond distances (0.93–0.98 Å in the temperature range of 183–243 K). Complexes **15** and **17** have the PPh_3 ligand in place of the IMes ligand. IMes is a strong sigma donor as compared to PPh_3. In addition, IMes is sterically bulkier than PPh_3. As it was discussed earlier, presence of the bulky IMes ligand in complexes **6–7** imposes steric

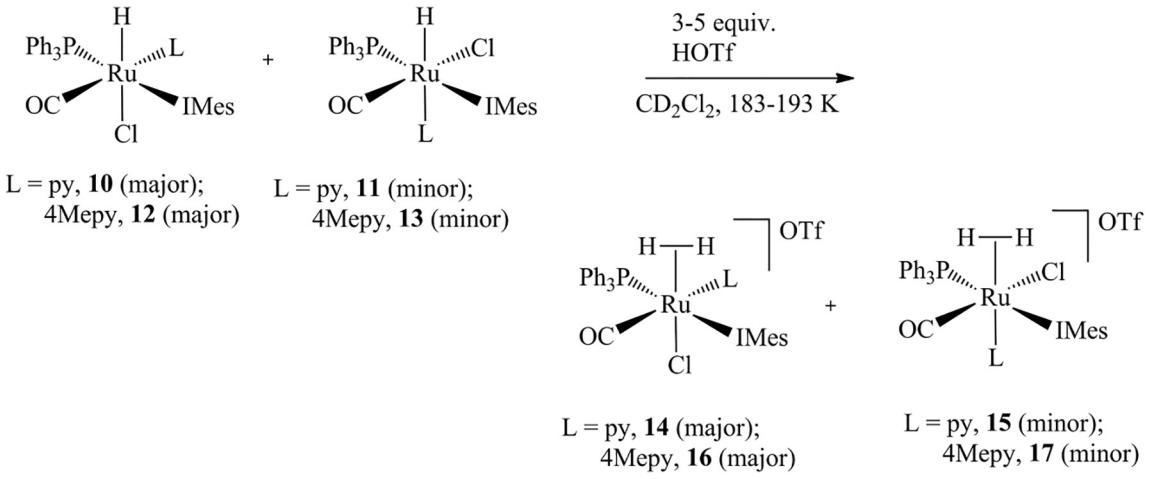

L = py, **10** (major); 4Mepy, **12** (major)

L = py, **11** (minor); 4Mepy, **13** (minor)

L = py, **14** (major); 4Mepy, **16** (major)

L = py, **15** (minor); 4Mepy, **17** (minor)

Scheme 8. Synthesis of ruthenium dihydrogen complexes bearing phosphine ligands.

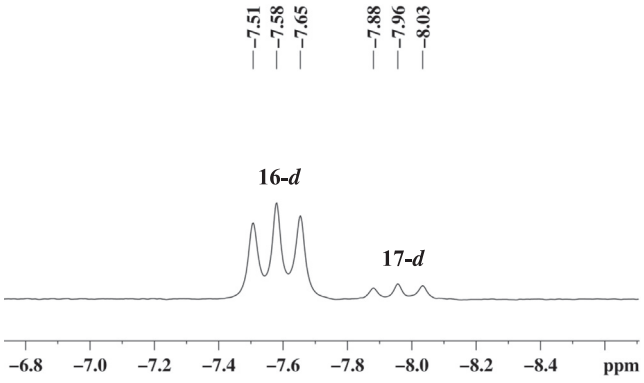

Fig. 9. Partial ^{1}H NMR spectral signal for the η^2-HD ligand of [RuCl(η^2-HD)(CO)(PPh_3)$_2$(4Mepy)]OTf (*trans*, **16-*d*;** and *cis*, **17-*d***) in CD_2Cl_2 at 223 K.

crowding around the Ru(II) center which renders their trans ligands to be labile. Thus, the temperature dependent nature of the H−H bond distance is a manifestation of the labile nature of the sterically bulky IMes ligand in complexes **6–7**.

4. Conclusions

We reported the synthesis and characterization of several dihydrogen complexes bearing an *N*-heterocyclic carbene ligand [RuCl(η^2-H_2)(CO)(IMes)(PPh_3)(L/L′)][OTf] (L = py, **6**; 4Mepy, **7**; L′ = MeCN, **8**; Me_3CCN, **9**) and dihydrogen complexes bearing phosphine ligands [RuCl(η^2-H_2)(CO)(PPh_3)$_2$(L)](OTf) [L = py, **14/15**; 4Mepy, **16/17**]. The H−H bond distances of η^2-H_2 ligand in all the dihydrogen complexes were calculated from the $^{1}J_{HD}$ values. Small, yet significant variations in the H−H distances from 0.98 Å to 0.93 Å in dihydrogen complexes bearing an N-heterocyclic carbene ligand **6–9**, were noted in the temperature range 193–243 K. The H−H distances in phosphine dihydrogen complexes **15** and **17** were found to be 0.93 Å and the d_{HH} was invariant at all the temperatures (193–263 K). Similarly, H−H distances in **14** and **16** were found to be about 0.95–0.96 Å. The H−H distances obtained here for all the dihydrogen complexes suggest that they belong to true dihydrogen complexes category. However, the H−H distances in complexes **6–9** are temperature-dependent which increases from 0.93 to 0.98 Å in the temperature range 243–193 K. The findings of this study suggest that the bulky IMes in the dihydrogen complexes **6–9** impose steric crowding around the Ru(II) center which makes these *trans* ligands labile. Thus, the temperature-dependent nature of the H−H distance in complexes **6–9** is a manifestation of the lability of the *trans* ligands rendered by its (IMes) steric bulkiness. The present study has shown the role of IMes and *trans* ligands in a series of dihydrogen complexes. This study has several implications to understand the chemistry of dihydrogen complexes bearing an N-heterocyclic carbene ligand for further research.

Acknowledgements

We gratefully acknowledge financial support from the Science & Engineering Research Board, (SERB) of India. D.M. thanks the Council of Scientific & Industrial Research (CSIR) of India for a fellowship.

Author contributions

The manuscript was written through contributions of all authors.

Appendix A. Supplementary data

Supplementary data associated with this article can be found, in the online version, at https://doi.org/10.1016/j.ica.2018.08.015.

References

[1] (a) M. Bardají, A.-M. Caminade, J.-P. Majoral, B. Chaudret, Organometallics 16 (1997) 3489;
(b) S. Burling, G. Kociok-Köhn, M.F. Mahon, M.K. Whittlesey, J.M.J. Williams, Organometallics 24 (2005) 5868;
(c) M.H.G. Prechtl, Y. Ben-David, D. Giunta, S. Busch, Y. Taniguchi, W. Wisniewski, H. Görls, R.J. Mynott, N. Theyssen, D. Milstein, W. Leitner, Chem. Eur J. 13 (2007) 1539;
(d) V.L. Chantler, S.L. Chatwin, R.F.R. Jazzar, M.F. Mahon, O. Saker, M.K. Whittlesey, Dalton Trans. (2008) 2603;
(e) N.J. Beach, J.M. Blacquiere, S.D. Drouin, D.E. Fogg, Organometallics 28 (2009) 441;
(f) S. Kern, R. van Eldik, Inorg. Chem. 51 (2012) 7340;
(g) S. Ramakrishnan, K.M. Waldie, I. Warnke, A.G. De Crisci, V.S. Batista, R.M. Waymouth, C.E.D. Chidsey, Inorg. Chem. 55 (2016) 1623.
[2] C.P. Lau, S.M. Ng, G. Jia, Z. Lin, Coord. Chem. Rev. 251 (2007) 2223–2237.
[3] (a) U.L. Dharmasena, H.M. Foucault, E.N. dos Santos, D.E. Fogg, S.P. Nolan, Organometallics 24 (2005) 1056;
(b) W.N.O. Wylie, A.J. Lough, R.H. Morris, Organometallics 30 (2011) 1236.
[4] (a) A. Comas-Vives, G. Ujaque, A. Lledós, Organometallics 26 (2007) 4135;
(b) G. Jia, C.-P. Lau, Coord. Chem. Rev. 190–192 (1999) 83;
(c) R.H. Morris, Chem. Rev. 116 (2016) 8588.
[5] (a) R.H. Morris, J.F. Sawyer, M. Shiralian, J. Zubkowski, J. Am. Chem. Soc. 107 (1985) 5581;
(b) R.H. Crabtree, Acc. Chem. Res. 23 (1990) 95;
(c) P.G. Jessop, R.H. Morris, Coord. Chem. Rev. 121 (1992) 155;
(d) D.M. Heinekey, W.J. Oldham, Chem. Rev. 93 (1993) 913;
(e) P.A. Maltby, M. Schlaf, M. Steinbeck, A.J. Lough, R.H. Morris, W.T. Klooster, T.F. Koetzle, R.C. Srivastava, J. Am. Chem. Soc. 118 (1996) 5396;
(f) M. Schlaf, A.J. Lough, P.A. Maltby, R.H. Morris, Organometallics 15 (1996) 2270;
(g) G.J. Kubas, Proc. Natl. Acad. Sci. 104 (2007) 6901–6907.
[6] (a) R.H. Morris, Coord. Chem. Rev. 252 (2008) 2381;
(b) S. Dutta, Comptes Rendus Chimie 14 (2011) 1029.
[7] (a) S. Dutta, B.R. Jagirdar, M. Nethaji, Inorg. Chem. 47 (2008) 548;
(b) M. Findlater, K.M. Schultz, W.H. Bernskoetter, A. Cartwright-Sykes, D.M. Heinekey, M. Brookhart, Inorg. Chem. 51 (2012) 4672;
(c) R.H. Crabtree, Chem. Rev. 116 (2016) 8750.
[8] (a) B.R. James, A. Pacheco, S.J. Rettig, I.S. Thorburn, R.G. Ball, J.A. Ibers, J. Molecul. Catal. 41 (1987) 147;
(b) E.P. Cappellani, S.D. Drouin, G. Jia, P.A. Maltby, R.H. Morris, C.T. Schweitzer, J. Am. Chem. Soc. 116 (1994) 3375;
(c) M. Grellier, L. Vendier, S. Sabo-Etienne, Angew. Chem. Int. Ed. 46 (2007) 2613;
(d) G. Alcaraz, M. Grellier, S. Sabo-Etienne, Acc. Chem. Res. 42 (2009) 1640;
(e) N. Mathew, B.R. Jagirdar, R.S. Gopalan, G.U. Kulkarni, Organometallics 19 (2000) 4506.
[9] A.J. Arduengo, R.L. Harlow, M. Kline, J. Am. Chem. Soc. 113 (1991) 361–363.
[10] (a) M.N. Hopkinson, C. Richter, M. Schedler, F. Glorius, Nature 510 (2014) 485;
(b) C.M. Crudden, D.P. Allen, Coord. Chem. Rev. 248 (2004) 2247–2273.
[11] D. Giunta, M. Hölscher, C.W. Lehmann, R. Mynott, C. Wirtz, W. Leitner, Adv. Synth. Catal. 345 (2003) 1139–1145.
[12] (a) Y. Jiang, O. Blacque, T. Fox, C.M. Frech, H. Berke, Organometallics 28 (2009) 5493;
(b) M.A. Esteruelas, F.J. Fernández-Alvarez, E. Oñate, Organometallics 26 (2007) 5239;
(c) G.E. Dobereiner, A. Nova, N.D. Schley, N. Hazari, S.J. Miller, O. Eisenstein, R.H. Crabtree, J. Am. Chem. Soc. 133 (2011) 7547;
(d) M. Baya, B. Eguillor, M.A. Esteruelas, M. Oliván, E. Oñate, Organometallics 26 (2007) 6556;
(e) S. Burling, L.J.L. Häller, E. Mas-Marzá, A. Moreno, S.A. Macgregor, M.F. Mahon, P.S. Pregosin, M.K. Whittlesey, Chem-Eur J. 15 (2009) 10912;
(f) P. Buskens, D. Giunta, W. Leitner, Inorg. Chim. Acta 357 (2004) 1969.
[13] B. Chin, A.J. Lough, R.H. Morris, C.T. Schweitzer, C. D'Agostino, Inorg. Chem. 33 (1994) 6278.
[14] D. Mala, B.R. Jagirdar, Y.P. Patil, M. Nethaji, J. Organomet. Chem. 830 (2017) 203.
[15] (a) A.J. Arduengo III, R. Krafczyk, R. Schmutzler, H.A. Craig, J.R. Goerlich, W.J. Marshall, M. Unverzagt, Tetrahedron 55 (1999) 14523;
(b) X. Bantreil, S.P. Nolan, Nat. Protocols 6 (2011) 69.
[16] N. Ahmad, J.J. Levison, S.D. Robinson, M.F. Uttley, E.R. Wonchoba, G.W. Parshall, Inorg. Synth. John Wiley & Sons, Inc., 2007.
[17] (a) L. Farrugia, J. Appl. Crystallogr. 30 (1997) 565;
(b) G. Sheldrick, Acta Crystallogr. Sect. A 64 (2008) 112.
[18] (a) J.G. Małecki, Polyhedron 30 (2011) 79;
(b) J.G. Małecki, A. Maroń, Polyhedron 30 (2011) 1225;
(c) L. Maity, S. Das, A. Adhikary, H.K. Mondal, A.A. Kisan, S. Isab, J Dinda Goswami, Inorg. Chim. Acta (2018) in press;
(d) M.A. Esteruelas, S. Fuertes, M. Oliván, E. Oñate, Organometallics 28 (2009) 1582.
[19] (a) A.J. Arduengo III, S.F. Gamper, M. Tamm, J.C. Calabrese, F. Davidson, H.A. Craig, J. Am. Chem. Soc. 117 (1995) 572;
(b) C. Lorber, L. Vendier, Dalton Trans. (2009) 6972.
[20] K.P. Chiang, P.M. Barrett, F. Ding, J.M. Smith, S. Kingsley, W.W. Brennessel,

M.M. Clark, R.J. Lachicotte, P.L. Holland, Inorg. Chem. 48 (2009) 5106.
[21] J.P. Lee, Z. Ke, M.A. Ramírez, T.B. Gunnoe, T.R. Cundari, P.D. Boyle, J.L. Petersen, Organometallics 28 (2009) 1758.
[22] D.G. Hamilton, R.H. Crabtree, J. Am. Chem. Soc. 110 (1988) 4126.
[23] (a) I. Göttker-Schnetmann, D.M. Heinekey, M. Brookhart, J. Am. Chem. Soc. 128 (2006) 17114;
(b) R. Gelabert, M. Moreno, J.M. Lluch, A. Lledós, D.M. Heinekey, J. Am. Chem. Soc. 127 (2005) 5632;
(c) B.C. Mort, J. Autschbach, J. Am. Chem. Soc. 128 (2006) 10060;
(d) R. Gelabert, M. Moreno, J.M. Lluch, Chem-Eur J. 11 (2005) 6315;
(e) J.K. Law, H. Mellows, D.M. Heinekey, J. Am. Chem. Soc 123 (2001) 2085;
(f) J.K. Law, H. Mellows, D.M. Heinekey, J. Am. Chem. Soc. 124 (2002) 1024.